ARMY RESEARCH LABORATORY

Rebuilding and Modeling of a Thermal Radiation Source

Richard B. Loucks
Peter C. Muller
Richard L. Thane

ARL-TR-501 August 1994

NOTICES

Destroy this report when it is no longer needed. DO NOT return it to the originator.

Additional copies of this report may be obtained from the National Technical Information Service, U.S. Department of Commerce, 5285 Port Royal Road, Springfield, VA 22161.

The findings of this report are not to be construed as an official Department of the Army position, unless so designated by other authorized documents.

The use of trade names or manufacturers' names in this report does not constitute indorsement of any commercial product.

REPORT DOCUMENTATION PAGE

Form Approved
OMB No. 0704-0188

1. AGENCY USE ONLY (Leave blank)	2. REPORT DATE	3. REPORT TYPE AND DATES COVERED
	August 1994	Final, October 1988 - December 1993

4. TITLE AND SUBTITLE

Rebuilding and Modeling of a Thermal Radiation Source

5. FUNDING NUMBERS

4G061-405-U2

6. AUTHOR(S)

Richard B. Loucks, Peter C. Muller, and Richard L. Thane

7. PERFORMING ORGANIZATION NAME(S) AND ADDRESS(ES)

U.S. Army Research Laboratory
ATTN: AMSRL-WT-NC
Aberdeen Proving Ground, MD 21005-5066

8. PERFORMING ORGANIZATION REPORT NUMBER

9. SPONSORING/MONITORING AGENCY NAME(S) AND ADDRESS(ES)

U.S. Army Research Laboratory
ATTN: AMSRL-OP-AP-L
Aberdeen Proving Ground, MD 21005-5066

10. SPONSORING/MONITORING AGENCY REPORT NUMBER

ARL-TR-501

11. SUPPLEMENTARY NOTES

12a. DISTRIBUTION/AVAILABILITY STATEMENT

Approved for public release; distribution is unlimited.

12b. DISTRIBUTION CODE

13. ABSTRACT (Maximum 200 words)

This report describes improvements to a U.S. Army Research Laboratory Thermal Radiation Source (TRS). This TRS unit is an aluminum powder/liquid oxygen torch incorporating a tailored combustion chamber to flatten the flame and is intended to be installed in the ARL 2.44-m shock tube. The combination of a TRS within a shock tube will provide the Army a facility for modeling a larger facility, conducting blast/thermal synergism experiments, and testing nuclear survivability of military equipment, components, and materials. Modifications made to the original TRS included installation of a new divert valve, change in the aluminum tank pressurization and aeration system, and pneumatic actuators. These changes significantly raised the radiation level and stability. A major operational change was computer control over the TRS sequence timer and data acquisition system. Parts of the TRS have been mathematically modeled. Methods to characterize the radiation output are described.

14. SUBJECT TERMS	15. NUMBER OF PAGES
nuclear explosion simulation, thermal radiation, heat transfer, heat conductivity, thermal conductivity, numerical analysis	72
	16. PRICE CODE

17. SECURITY CLASSIFICATION OF REPORT	18. SECURITY CLASSIFICATION OF THIS PAGE	19. SECURITY CLASSIFICATION OF ABSTRACT	20. LIMITATION OF ABSTRACT
UNCLASSIFIED	UNCLASSIFIED	UNCLASSIFIED	SAR

Intentionally left blank

ACKNOWLEDGMENTS

The author wishes to express his gratitude for the advice and work of Dr. John Polk at the U. S. Army Research Laboratory (ARL). He was essential in correcting the calorimetric data. Appendix C contains his contribution. Another contributor is Dr. Pat Kingman of ARL who provided extensive micrographs and analysis of the aluminum powder, and her work is in Appendix D. The author also appreciates the technical review of Mr. John Sullivan, whose efforts were not only beneficial to the paper, but an education for the author.

Intentionally Left Blank

TABLE OF CONTENTS

Intentionally left blank

LIST OF FIGURES

1. INTRODUCTION

With the ban of aboveground nuclear testing, it has been impossible to accomplish performance testing on military equipment in a nuclear environment. Within the past 30 yr, several nuclear simulators have been constructed to accomplish this testing. Recently, technology has made feasible the construction of a simulator of nuclear air blast and thermal loading called the Large Blast/Thermal Simulator (LB/TS).

To support the design of this facility, the Blast/Thermal Effects Branch of the U.S. Army Research Laboratory (ARL) has been working with an aluminum powder/liquid oxygen Thermal Radiation Source (TRS) system. Once it was optimized, the TRS unit was to be installed in the ARL 2.44-m shock tube. In this fashion, problems arising with the LB/TS could be studied on a smaller, less expensive scale.

The current TRS incorporates numerous modifications from its original state. It uses aluminum powder reacting with liquid oxygen (LOX) in a combustion chamber to create a large fan-like flame. The flame acts as a large thermally radiant wall, which simulates the nuclear thermal radiation pulse delivered to a target. The flame is so shaped to give a more uniform radiating area in the confined area of the shock tube.

In the original TRS, the thermal output of the flame oscillated with large amplitude relative to the mean yield. It was speculated that a fluctuating mass flow rate of aluminum powder in the system caused the unstable output. There was no control over the thermal output relative with time except for initiation and termination of the source. The rise and fall rate of thermal output was slow and inconsistent. All of these factors led to poor prediction of the output, rendering the TRS an ineffective simulator.

An attempt was made to control the thermal output to match a true nuclear thermal pulse. A true nuclear thermal pulse has a rapid rise with a slower tail-off, as shown in Figure 1. Control of the TRS output was tried with a computer-controlled aluminum divert valve. The effort failed due to aluminum powder clogging the moving parts of the valve and slowing or stopping the motion.

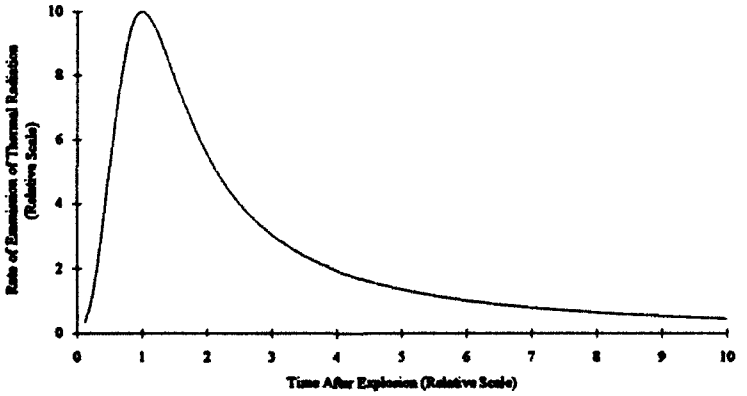

Figure 1. Nuclear thermal pulse profile, relative scale.

Modifications were made to the original TRS unit to improve its performance. The modifications included: changing the divert valve to a three-port ball valve, adding a custom-built combustion chamber, improving LOX and aluminum mixing, and making changes to the pneumatic and transport process. The combustion chamber improved the LOX/aluminum mixing as well as spreading the flame over a greater area. The divert valve operation was changed to produce a "rectangular" thermal pulse. The ball valve was selected to divert aluminum to and from the combustion chamber for faster rise and fall times on the flux record. There still existed a large fluctuation in the thermal output.

An engineering model of the aluminum powder pressure vessel was constructed in the hope that it would show the cause of the large thermal fluctuations. The actual output of the model was mass flow rate of aluminum from the exit given the inlet gas pressures. The model did reveal the source of mass flow fluctuations was not directly due to the existing pneumatic setup. The fluctuations were shown when assumed to be caused by forces outside the pressure vessel. Once the outside disturbance was eliminated, the model demonstrated a low transient flow rate of aluminum powder. The results were applied to the TRS, and the thermal output was stabilized.

Modifying the system delivering aluminum to the nozzle created smoother and higher flux records. These changes significantly improved the system's output and performance. These technology upgrades could also be applied to the TRS system designated for the LB/TS to assure favorable operation.

2. ORIGINAL THERMAL RADIATION SOURCE

In 1976, the branch (then the Blast Dynamics Branch of the Ballistic Research Laboratory) purchased an aluminum powder/liquid oxygen TRS. This unit, along with a set of three combustion products ejectors, was to be integrated into the ARL 2.44-m shock tube. For evaluation, both systems were installed in a 2.44-m pipe section.

The TRS unit was composed of two parts, the module or "fuel skid," and the three nozzles, as shown in Figure 2. The module contained the pressure vessels that held the aluminum powder and LOX. It stored the high pressure nitrogen used to operate the TRS. It contained all regulators and pressure gauges and was also the electrical junction for the valve actuators. The nozzles were a separate body placed 10 m from the module. At the nozzles, aluminum powder and LOX were mixed and ejected into the air vertically. The nozzle exit was a small steel combustion chamber lined with 3 cm of graphite. A propane/oxygen cross flame covered the nozzle exit into the chamber and ignited the passing aluminum/LOX mixture.

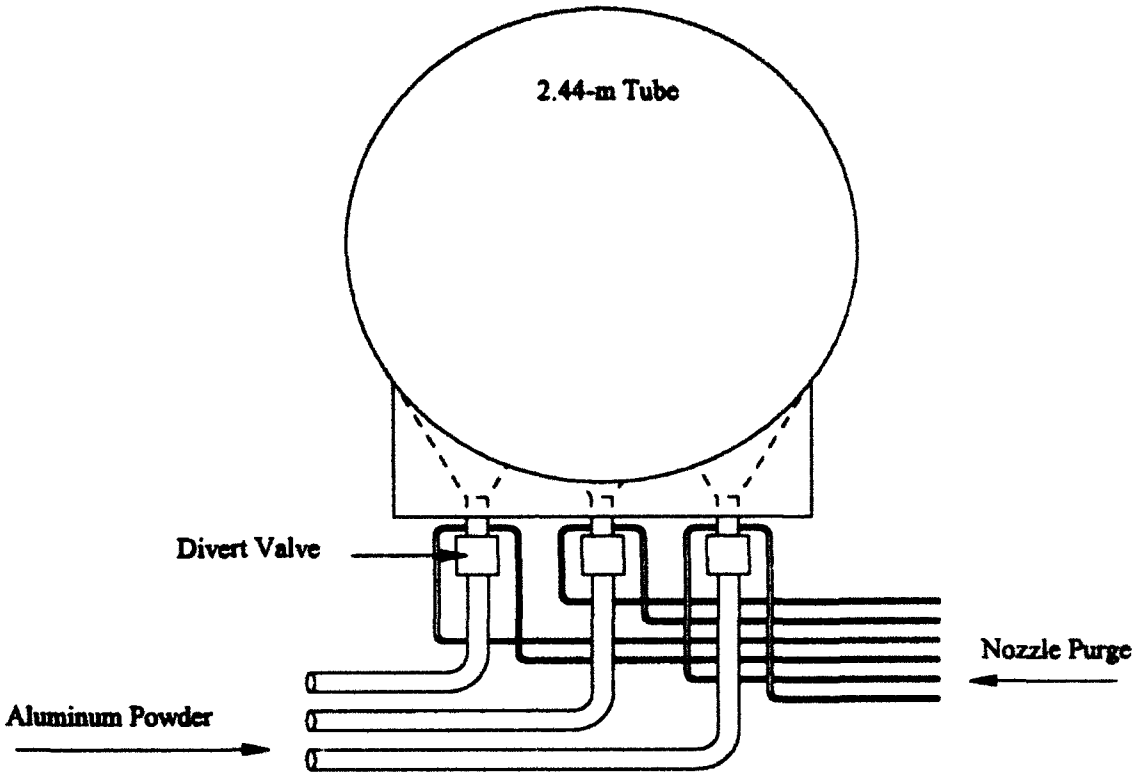

Figure 2. Three-nozzle TRS .

The TRS failed on its first trial, destroying one of the nozzles. The problem encountered with the three-nozzle unit was a faulty seal between the ignition ports and the combustion chamber. The seal failure allowed hydrogen and oxygen gas to jet out the side of the nozzle. The ignited flame acted as a blow torch, melting many of the middle nozzle components. The process of the degrading nozzle and the continued combustion of aluminum powder and LOX caused the complete de· ·uction of the middle nozzle and the right nozzle. The left nozzle was left without damage, later to be salvaged into an improved TRS unit. This event severely hampered the TRS program at ARL. Aluminum/oxygen TRS work was considered to be difficult to control and unsafe.

2.1 Aluminum Powder and LOX System.

The aluminum powder and oxygen are jetted into the air at an initial velocity of about 15 m/s. The majority of the thermal radiation generated from the aluminum/LOX TRS is from the condensing particles of alumimum oxide (Rehmann 1983). The ignition flame serves as a catalyst to cause a rapid reaction between the aluminum powder and oxygen-rich environment. The ignition flame melts off a very thin aluminum oxide shell which exist on all aluminum particles. The melting temperature for aluminum oxide, 600 K, is much higher than

that of pure aluminum. When the aluminum oxide shell is melted, the aluminum is quickly melted and reacts strongly with the oxygen-rich environment. The reaction itself generates heat and becomes self propagating. When the reaction is complete, the resulting aluminum oxide is in the vapor phase. Convective heat transfer causes the aluminum oxide vapor to cool and condense at about 3,000 K. The latent heat released from the phase change and the resulting radiant heat released from the aluminum oxide molten mist account for the majority of the heat radiation. Eventually, the molten aluminum oxide radiates enough heat and cools to the solid phase. At this point, there is little radiant energy coming form the particles, and the heat transfer mechanism is mostly convective. This process creates a large flame radiating at a high temperature.

In the original TRS, control of the aluminum powder and LOX flow to the nozzles was accomplished with pressurized nitrogen gas. The aluminum powder tank and LOX tank pressures were preset by their respective nitrogen regulators. When a ball valve at the bottom of the aluminum powder tank opened, the aluminum powder was injected into a nitrogen gas high-speed line. A divert valve in the nozzle switched the aluminum flow either to the waste recovery bin or to the combustion chamber. LOX was driven by pressurized nitrogen gas to the nozzle. Both LOX and aluminum powder would flow during the entire operation.

The aluminum was contained under pressure in a steel cylinder that has a two-way ball valve on the bottom. The bottom part of the valve injected into a Venturi chamber and was mixed with passing high-speed nitrogen, as depicted in Figure 3. This was where the high-pressure nitrogen expanded at high speed. The static pressure was less than the pressure in the aluminum tank. When the valve opened, aluminum was forced into the high-speed line by the nitrogen pressure and aluminum weight. It was entrained with the high-speed nitrogen and accelerated towards the nozzle.

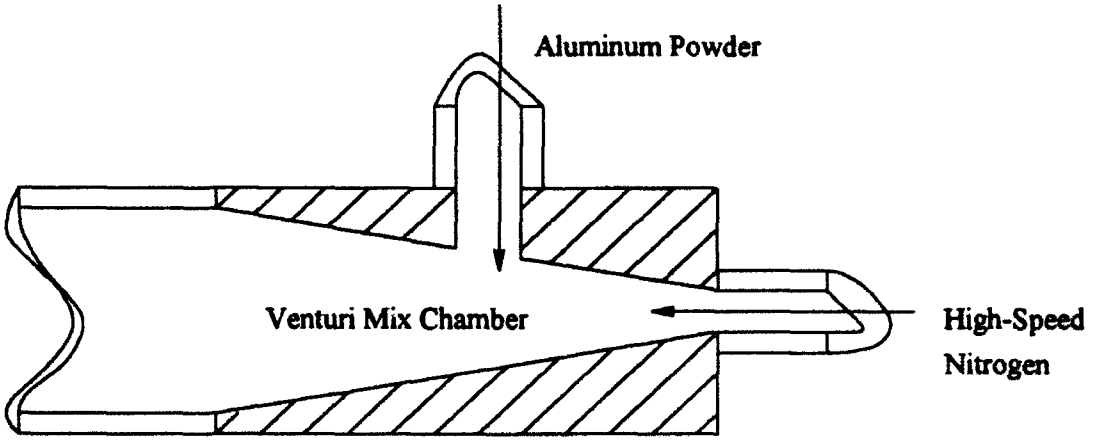

Figure 3. Aluminum powder in venturi mixing chamber.

The aluminum powder and LOX were transported 10 m to the nozzle. The LOX would flow directly to a mixing chamber and out the combustion chamber. When the divert valve changed the aluminum flow from the waste recovery bin, aluminum met LOX in the mixing chamber. The mixture was ejected into the combustion chamber past the propane/oxygen cross flame. The valves were operated by gas driven actuators that responded to

a 24-V signal from a sequence timer. The voltage would energize the solenoid that would open a gas valve within the actuator piston chamber. The gas would displace the piston, mechanically moving the valve by a rack and pinion linkage.

2.1.1 The Aluminum Powder.

The aluminum powder used at ARL is Reynolds Aluminum grade 120. As seen in Figure 4, the particles range in size from less than 1 μm to 100 μm. The average particle size is about 18 μm, using the Fisher method (Reynolds Aluminum 1990). The particles are not spherical due to the manufacturing process. A spherical grade can be used, but this granular form is probably superior due to the increased surface-to-volume ratio for reaction.

Figure 4. Grade 120 aluminum powder heterogeneous region at 500X.

To assess the average particle size, several micrographs using a scanning electron microscope were taken at different magnifications. In evaluating the micrographs, no quantitative conclusion could be drawn as to the size distribution. The sample drawn from the lot could be made to vary, since the distribution of powder within the lot was not homogeneous. Furthermore, the method of removing a small sample could bias the final distribution. In addition, the sample handling method strongly influenced the particle distribution in the final amount. The micrographs did provide an understanding of the range in particle sizes. For more details, refer to Appendix D.

The Reynolds Aluminum grade 120 is the only type of aluminum powder currently used at ARL. In September 1989, the same grade was used by Science Applications International Corporation (SAIC) when

performing the acceptance tests on a four-nozzle TRS called "SATAN" for the Centre d'Etudes de Gramat (CEG) in Gramat, France. The test, performed at SAIC Laguna Test Site, New Mexico, yielded acceptable results. When the TRS system was reassembled in Gramat, France, the output of the TRS was obviously different (Mergnat 1990). Without immediate access to Reynolds Aluminum grade 120, the CEG used a local supplier of aluminum powder. Based on what SAIC had specified for aluminum size, the CEG purchased aluminum powder with an average particle size of 20 μm. Apparently, the European supplied aluminum powder had a much tighter distribution of particle size. The thermal output of SATAN was much lower than expected, with the flux level increasing with time.

The CEG changed the aluminum to a much larger particle size, 80 μm. The effect was the complete opposite, with a high initial flux but decreasing with time. The members at CEG combined equal amounts of the two grades and were able to achieve the same results at the SAIC Laguna Test Site. Since it is evident that the grade of aluminum will affect the thermal output, Reynolds grade 120 was selected as the control fuel for TRS experiments.

2.1.2 LOX.

The LOX was pressurized in an insulated container with nitrogen gas to drive it through the nozzle piping. The 50-gal LOX tank was insulated to maintain the cryogenic temperatures necessary and minimize losses. Initially, the LOX flow was started as soon as the sequence count began. The lead time let the flow cool the nozzle plumbing, thereby minimizing LOX evaporation during the event. When the LOX arrived at the three nozzles, it evaporated while mixing with the aluminum particles. The oxygen-rich mixture was ejected past the propane/oxygen flame and began burning within the combustion chamber.

2.2 Divert Valve.

A divert valve in line with each nozzle controlled the direction of aluminum flow. The aluminum would flow either to the waste recovery bin or to the nozzle. At the start of TRS operation, the aluminum powder flowed to the waste recovery bin for a few seconds, then would divert into the nozzle, then back to the waste recovery bin.

The divert valve, depicted in Figure 5, was a dual-plunger assembly. The aluminum powder would be transported into the chamber where a nylon wedge would divert the flow of aluminum to the open exit port facing the vertical. Depending on which plunger was up or down determined which path the aluminum would take. The plungers were actuated by a computer-controlled stepper motor. The stepper motor was used to try to control the aluminum mass flow such that the TRS would simulate the flux history of a nuclear event as shown before in Figure 1.

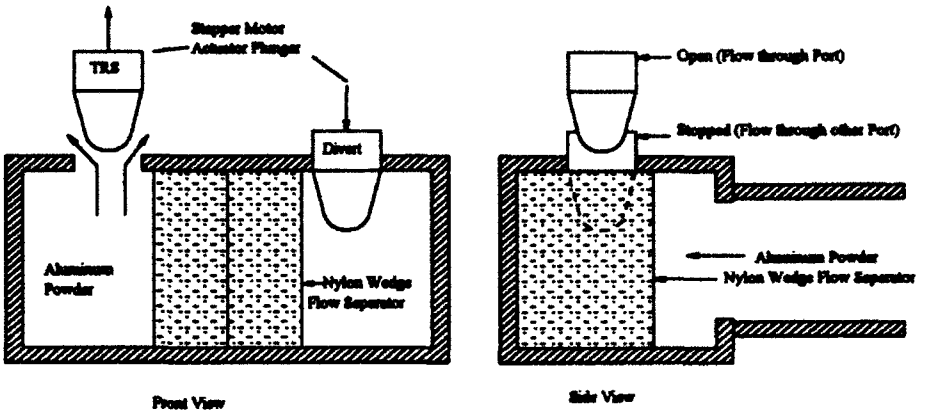

Figure 5. Plunger divert valve.

This valve design was the primary cause of the TRS failure. As aluminum powder entered into the valve, many of the moving parts were impeded by the aluminum dust. The valve of one nozzle stopped functioning in the middle of a test, leaving the aluminum and LOX mixture to flow and burn without control. The steel and graphite combustion chamber eventually melted, damaging several components of the nozzle. Aluminum slag from the unrestrained burn contributed to the damage of the nozzle. The actuators, nitrogen gas lines, divert valve, and the structural framework were damaged beyond salvage.

3. MODIFICATIONS AND UPGRADES

To improve the simulator, ARL personnel generated a set of objectives for an improved TRS. The need for the TRS to reproduce the nuclear thermal pulse of Figure 1 was relaxed. A nuclear event radiates at an equivalent black body temperature of about 6,000 K, where the combustion products of the TRS radiate at about 3,000 K. Since the color spectrum was incorrect, there was no need to emulate the time profile of a true nuclear thermal pulse. An easily controlled "rectangular" thermal pulse was chosen for the TRS, matching the total radiant energy, or fluence, on the target. For maximum control, the new TRS would emit at its peak rate of thermal output within 100 ms from initiation. The flux, or thermal radiant intensity, would not vary by a standard deviation greater than 10% of the average output. The output was to be terminated within 100 ms after a desired fluence was achieved. The source was to be integrated with the 2.44-m shock tube, which has since been renamed the "probative tube." Operation of the TRS was to be safe and repeatable.

The TRS program was continued with the least damaged of the remaining TRS nozzles and the module. A single unit would be simpler to study than three at once. It would be modified, upgraded, and tested. One modification would be to change the combustion chamber to spread the flame. If the reshaped flame emitted mostly in one direction, it would give the same cover of uniform irradiance as three TRS nozzles.

3.1 Combustion Chamber.

Three combustion chambers were used in the original three-nozzle TRS. The resulting TRS test demonstrated the evacuators were incapable of removing all the combustion products in time for a blast test. A single TRS unit would reduce the combustion products to be handled. In contrast, one of the original combustion chambers would be too small to generate a uniform thermal field within the 2.44-m probative tube. A larger combustion chamber that would spread the flame across the shock tube cross section was fabricated and installed.

The new combustion chamber mixed the LOX and aluminum powder differently than the original. The original method was to fill an outer sleeve with LOX and mix it with the aluminum as it passed by, as seen in Figure 6. The mixture would enter the combustion chamber, ignite, and jet upward. The LOX sleeve was not a good design since the aluminum would sometimes enter the sleeve and would burn after the event was over. Burning in the sleeve was part of the reason the original TRS was damaged.

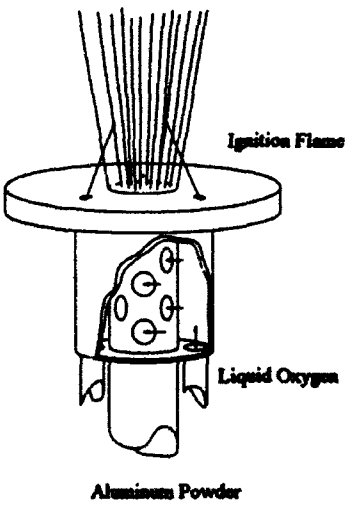

Figure 6. Mixing chamber and LOX/aluminum mixing.

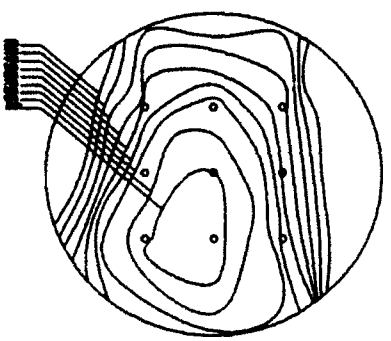

Figure 7. Contour plot of thermal mapping of TRS, 100 cm from TRS center.

The new method of mixing injected the LOX into the aluminum powder stream at an upward angle. To aid in the mixing and to prevent aluminum from entering the chamber, a nozzle purge system was installed. Nitrogen gas at high pressure was introduced into the aluminum powder flow, just before the aluminum mixed with the LOX. When the aluminum stopped flowing, the nitrogen would purge the area of any residual particles out into the chamber. The purge nitrogen helped propel the LOX-aluminum mixture through the igniters. It also prevented any molten residue from flowing back into the high-speed line.

The propane/oxygen ignition cross flame was replaced with a hydrogen/oxygen ignition system. The hydrogen and oxygen mixed in a small chamber, then ignited by an automotive spark plug. The flame was injected into the combustion chamber. The spark plug ignition method proved to be much more reliable than the furnace spark rods, and the hydrogen/oxygen burned hotter than the propane/oxygen ignition system.

The resulting fluence of the combustion chamber is shown in Figure 7. This thermal mapping shows a flaw in the combustion chamber output. The plane area of irradiation at 1 m from the nozzle center is not very uniform. There is a distinct high gradient flux region at the center lower part. Fortunately, the size of the targets in the probative tube are limited due to blockage effects. The typical target to be tested will be small with respect to this region, and will be affected in a fairly uniform manner. The small circles show the location of the calorimeters used during the test.

The resulting isotherm contours in Figure 7 were generated by using a matrix of fitted third-order polynomials and using a French curve to connect the grid intersections. A polynomial was fitted to the top three horizontal calorimeter values, corresponding to a line running through the calorimeter centers. Percent values in increments of ten, of the maximum calorimeter reading, were indicated along the curve. This procedure was repeated vertically, horizontally, and diagonally for all lines connecting three calorimeters. The resulting overlap of decade values were never apart by more than 5 cm, mostly no more than 2 cm. The result was a group of points representing the polynomial estimate of decade percentile values. A French curve was used to smoothly connect the isotherm points. The resultant contours yield an estimate of the energy distribution within the shock tube area.

The largest drawback of the combustion chamber is the accumulation of slag on the walls of the combustion chamber after each test. If the slag is not cleaned off after each test, the buildup of material will interfere with the flame, causing higher transient, less predictable output. Figures 8, 9, and 10 show in sequence the deterioration of TRS output with an unclean combustion chamber.

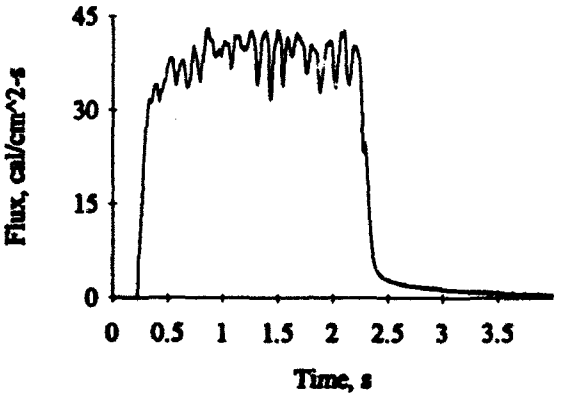

Figure 8. TRS output with clean combustion chamber.

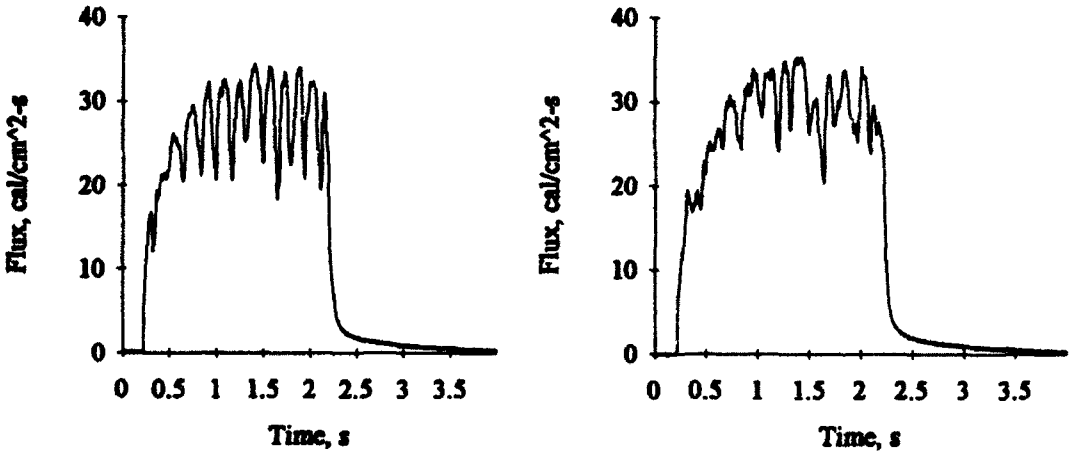

Figure 9. TRS output during 2nd and 3rd event.

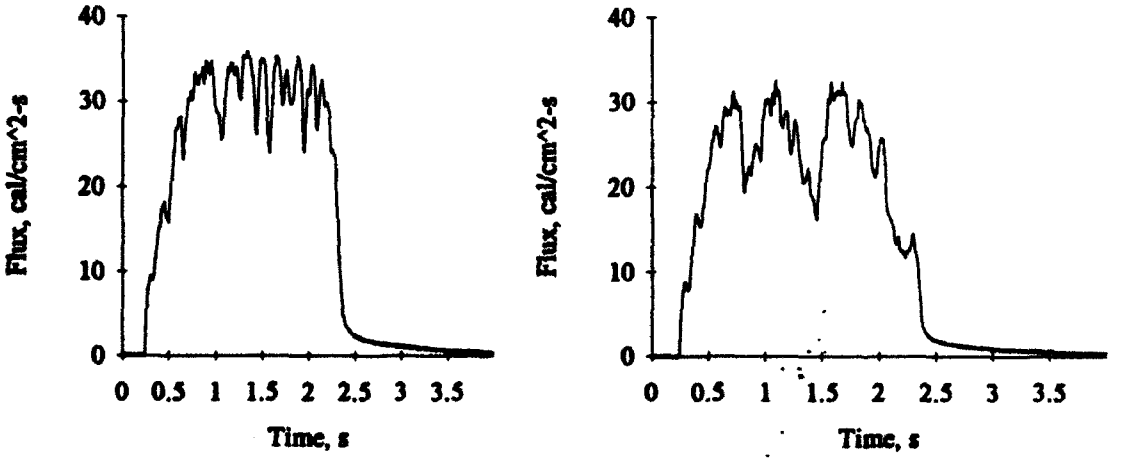

Figure 10. TRS output during 4th and 5th events.

3.2 New Divert Valve.

A three-port, bronze ball valve was selected for the modification of one of the remaining nozzles. The initial flow of aluminum would be turned at 90° in the ball valve and transported to a waste recovery bin. At the desired moment, the ball valve would turn 90°, diverting the aluminum flow into the combustion chamber. After a given time, the ball valve would be turned back to its original position, cutting off the TRS flame and allowing aluminum to flow back into the catch barrel. This sequence is shown in Figure 11.

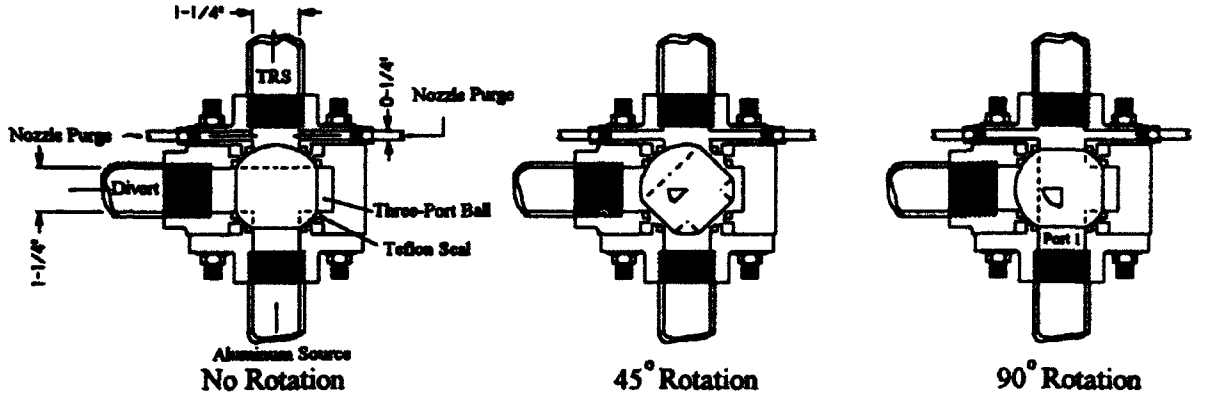

Figure 11. Three-port ball valve operation.

The three-port ball valve was installed in the retained nozzle, just behind the larger combustion chamber. A pipe with constant circular cross section in the 90° bend was added to smooth the flow of aluminum from a horizontal direction to the vertical direction. The trial test produced a thermal pulse of moderate rise time but sharp fall time, as seen in Figure 12. This result was progress toward the objective of a rectangular pulse. The high amplitude fluctuations are discussed in section 3.7.

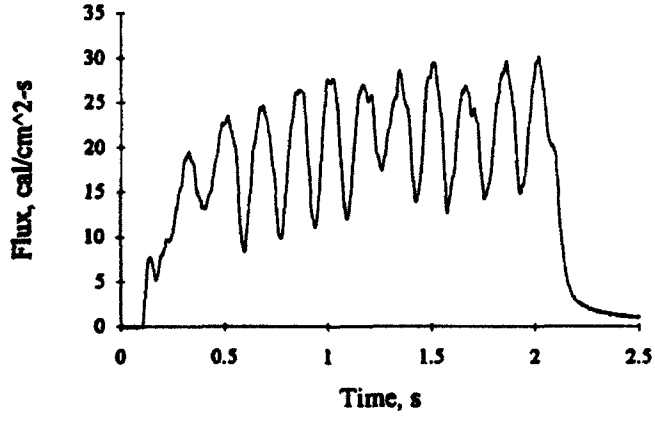

Figure 12. TRS flux record with three-port ball valve.

Residual aluminum powder not eliminated by post-test cleaning reacts over a period of time with the moisture in the atmosphere. The result is an extremely stiff, thick aluminum oxide buildup. The original divert valve was ruined by the effects of aluminum oxide buildup. There was concern that an oxide coating on the ball valve's moving parts would impede the rotation motion.

The valve was spot checked after each test. The ball valve actuator was tested with increments of pressure to determine the minimum pressure necessary to turn the ball. It was expected that as more TRS events occurred, aluminum oxide would build up, and the minimum actuator pressure would need to increase. However, after twenty events, there was no change in resistance; after forty events, the resistance was reduced.

The valve was disassembled for inspection and lubrication. The interior showed little residual aluminum powder. Most was captured by the valve lubricant. The ball surface showed little to no abrasion. The white nylon seals had turned gray in areas and actually reflected as polished aluminum in spots. It was concluded that the ball valve was working properly.

The apparent absence of aluminum was explained by the nature of how the valve operated. As the ball rotated, the nylon seals would clean the ball. The imperfections of the seals were filled with aluminum powder and were eventually compacted and polished with each event. As each event occurred, the ball experienced slight wear, accounting for the slight decrease in rotation resistance.

The basic advantage of the ball valve over the plunger valve system was that the ball valve had fewer moving parts. In the abrasive environment of aluminum powder and the possibility of buildup areas, decreasing the number of active parts was essential. A further advantage was that the ball valve had no spaces where aluminum could accumulate.

3.3 Control and Instrumentation.

One of the problems with the three-nozzle TRS was the lack of active control when the system was running. A programmed sequence timer took over operation after the TRS was started. It would run the entire event by energizing solenoids which in turn opened and closed pressure-actuated valves. With the uncertainty of the TRS operation, at least an abort mode needed to be added.

The TRS required improvements in the control and instrumentation. The primary sensor for the TRS flame was the Gardon-type flux sensor. The gauge output was recorded on an instrumentation quality tape recorder. The data from the tape would later be digitized on an analog-to-digital converter and processed on a computer to give fluence and an ink plot flux history. The data were stored in ASCII format on a data cartridge. Because the recording system was off-line and did no automatic processing, results and analysis were slow in coming.

3.4 Waste Recovery Bin.

The original waste recovery bin was designed to contain the diverted aluminum from three nozzles. The bin was designed to hold 60 kg of aluminum. The bin was simply a 55-gal drum with a modified lid. The lid was constructed with one entry port for the diverted aluminum and three 2.5-in pipes welded to the lid that ran vertically in the center of the barrel. The pipes were about 4 in from the bottom of the barrel and were about 2 in above the barrel lid. The "lips" of the pipes were used to attach commercial grade vacuum cleaner bags.

This system was extremely difficult to handle. Cleaning the barrel was difficult since the top had to be lifted with a hoist and the aluminum scooped out with a shovel. The pipes would get clogged with aluminum and retard flow through the bin. The obstruction caused the preflow of aluminum to be slow, sometimes causing slow rise times in thermal output.

The bin was improved by replacing the 55-gal drum with a smaller 10-gal container, as shown in Figure 13. The lid was changed to accept the aluminum divert and had one filtered exit port without any pipes. The incoming powder was directed against the wall and downward by a small sheet of aluminum just inside the entrance port. The filter was nothing more than a cloth rag stretched over the exit opening. This method is easier to handle, mainly because one man can lift the can with aluminum in it after each shot. The aluminum powder can be dumped back into the aluminum powder container at the TRS or be dumped back into the aluminum can for storage.

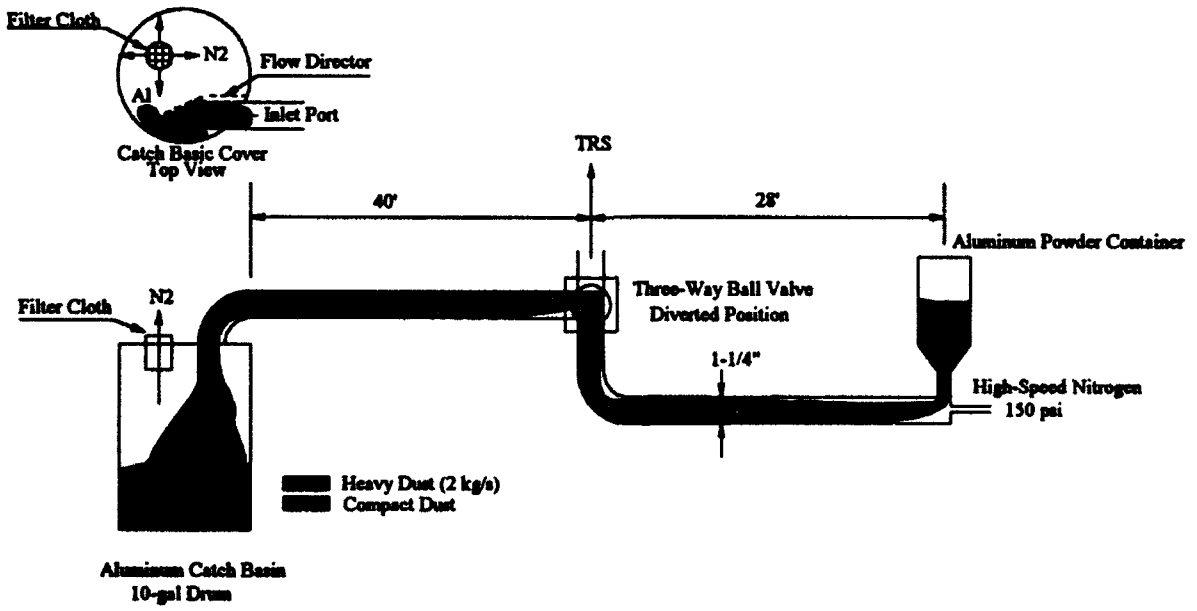

Figure 13. Improved waste recovery bin.

3.5 TRS Control Modification.

The sequence timer was replaced by a computer programmable controller. Initially, from a nearby station, a personal computer (PC) transmitted a basic time table to the on-site controller, as depicted in Figure 14. During the sequence run, the computer and controller would communicate. If certain key functions failed to occur, the controller would alert the computer and the operator, and either one could abort the run.

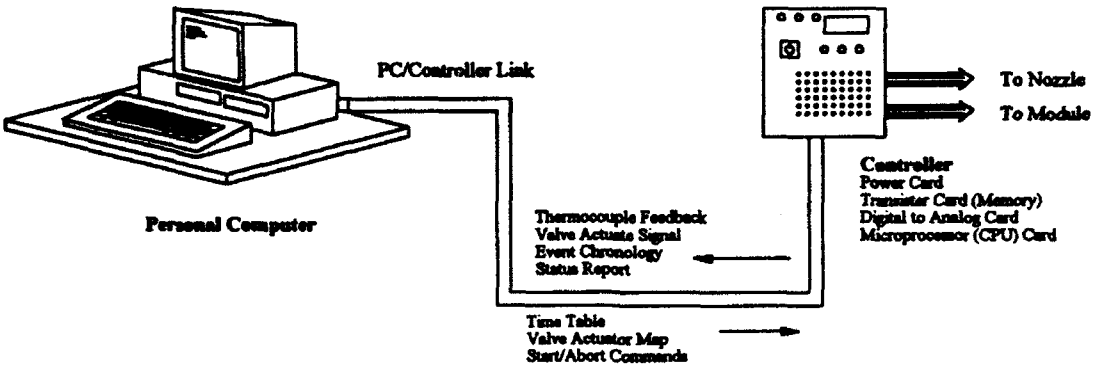

Figure 14. TRS controller and PC.

This new system allowed the experimenter to change the valve operation sequence and times with little effort. Its ease of programming and flexibility helped troubleshoot some major problems and helped eliminate misfires. For instance, improperly operating valves or actuators could be revealed by the controller feedback. Safe manual operation from the controller at the module could identify a problem component needing replacement.

The control system was instrumental in helping generate an operation checklist as detailed in Appendix A. With the reliability of the TRS control system improved, a standing operating procedure (SOP) for each TRS experiment was established. The SOP created a fundamental continuity of experimental procedure that was missing in past experiments.

The controller is made up of four integrated circuit cards — a power card, a CPU card, an analog card, and a transistor card. The power card distributes electrical power to the controller components. The CPU card exchanges data with the personal computer, reads the time tables from memory, and controls the TRS. The transistor card is the memory that holds the time table and the valve operation sequence. The analog card converts the digital CPU controller output into current for the proper actuator relays. The TRS controller is easy to repair. The four cards are easily removed and replaced. Controller to PC communication is attained by an RS-232 interface. The PC requires no additional special hardware. The controller is somewhat self-diagnostic. If one of the feedback sensors fails, the controller will not work and will indicate which sensor failed.

3.6 Instrumentation.

The Gardon-type gauge continued to be the principal calorimeter during the TRS testing. This was done to remove sensor influence and allow direct comparisons of new data to past data. The data acquisition system was modernized with a compact, sequential digital recorder that allowed up to 110 channels more than the tape recorder.

3.6.1 Calorimeters.

The Gardon type gauge is the primary transducer used to measure the flux output of the TRS. As sketched in Figure 15, the gauge is basically a constantan diaphragm welded to a copper wire and body. This particular construction generates two thermocouple junctions. The diaphragm acts as the heat transfer sensor while the main copper body acts as a heat sink.

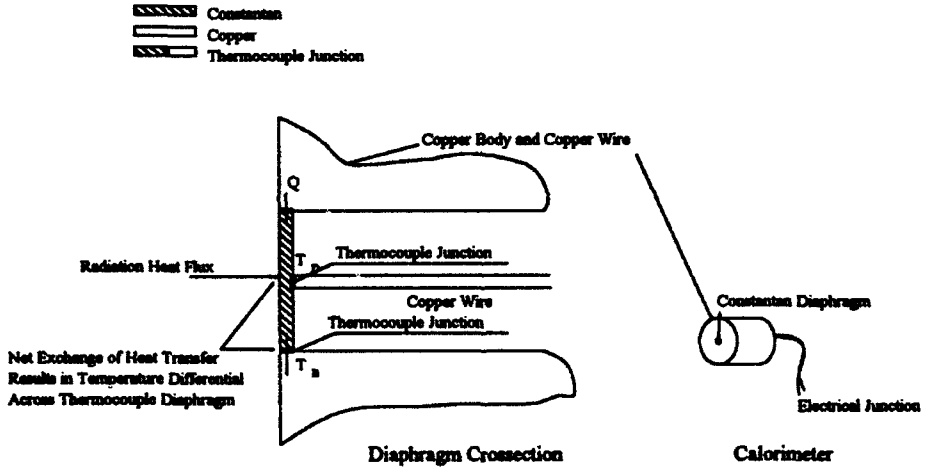

Figure 15. Gardon-type gauge for flux measurement.

The Gardon-type gauge, or calorimeter, produces a measurable voltage as a difference of temperature is produced between the two thermocouple junctions. This voltage can be represented as

$$V_m = C_{TC}(T_D - T_B),$$

where

V_m is the voltage produced from calorimeter

C_{TC} is a proportionality constant

T_D is the diaphragm center temperature

T_B is the diaphragm edge temperature.

This voltage signal, V_m, is recorded during the TRS event. A calibration constant is multiplied by the signal data to convert the data into engineering units. The calibration constant for each gauge is supplied by the manufacturer but is always checked at ARL against a National Bureau of Standards second-generation calibrated Gardon Gauge. The thermal radiation source for calibration is a graphite element heated by high voltage and current. The calibration is shown in Figure 16. The units of flux used at ARL are **calories per cm^2-second**.

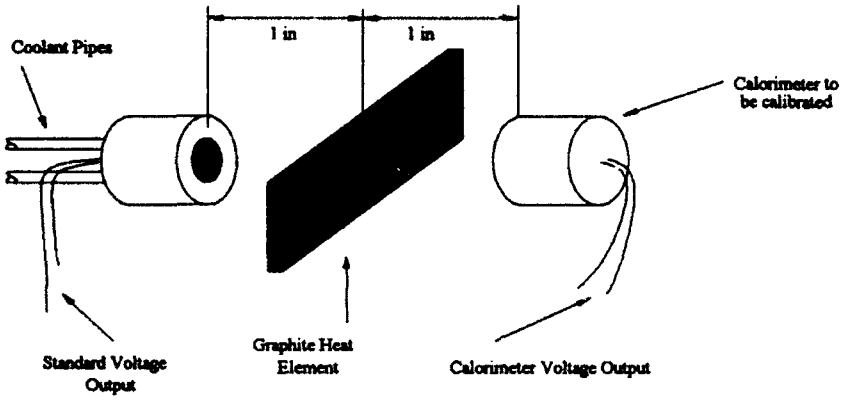

Figure 16. ARL calorimeter calibration technology.

One of the main concerns about these particular calorimetric data is the response time of the Gardon-type gauges (Loucks 1993). One manufacturer of this gauge claims an exponential response time of 68.2% within 50 ms. In other words, if the calorimeter experienced a discontinuity, it would respond to the signal as $(1-e^{-t/C_t})$, where C_t is the time constant and is equivalent to the reciprocal of the response time. If the TRS data traces are corrected using this number, there is an obvious difference in the flux trace, as seen in Figure 17. Details on this procedure can be found in Appendix B.

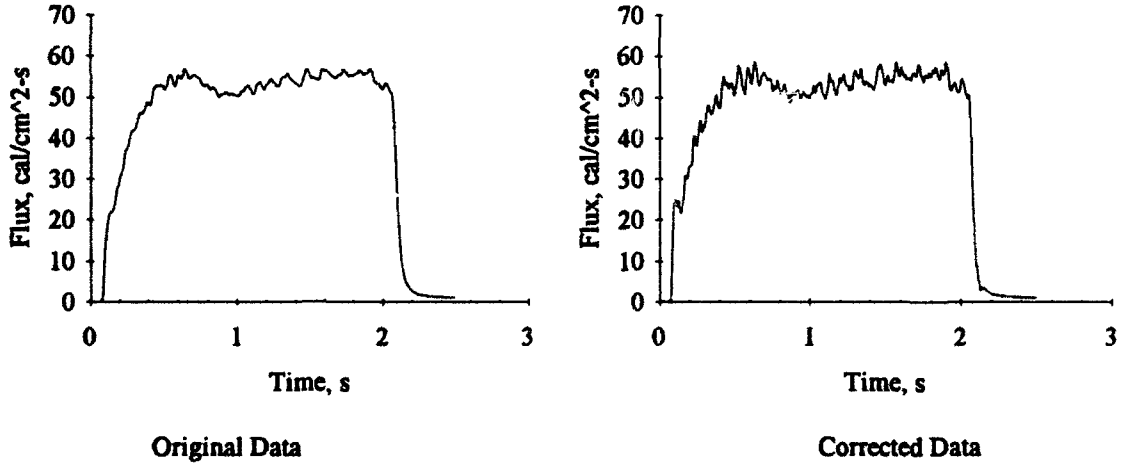

Figure 17. Flux history corrected for slow response time of sensor.

The flux history of Figure 17 shows the original measured trace and the flux history with a calculated correction for slow response time. The response time was determined from an experiment as sketched in Figure 18. Two calorimeters were placed side by side at the same elevation 1 m from the TRS center. One of the calorimeters had an aluminum plate covering the face so that all thermal energy from the TRS would be blocked. The plate was attached by a black thread. The TRS would burn the thread, allowing the aluminum plate to fall away from the calorimeter face. An approximate calculation shows the shutter time to full exposure to be about 1 ms, which is negligible when considering a response time of about 50 ms. The actual data generated from this experiment are shown in Figure 19.

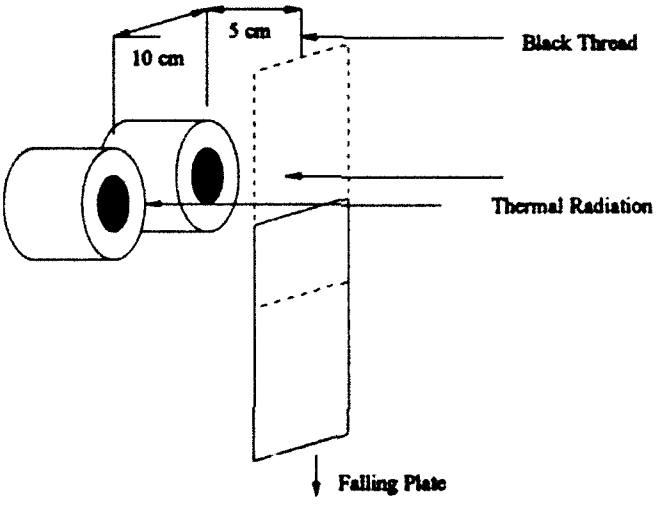

Figure 18. Calorimeter response experiment shutter setup.

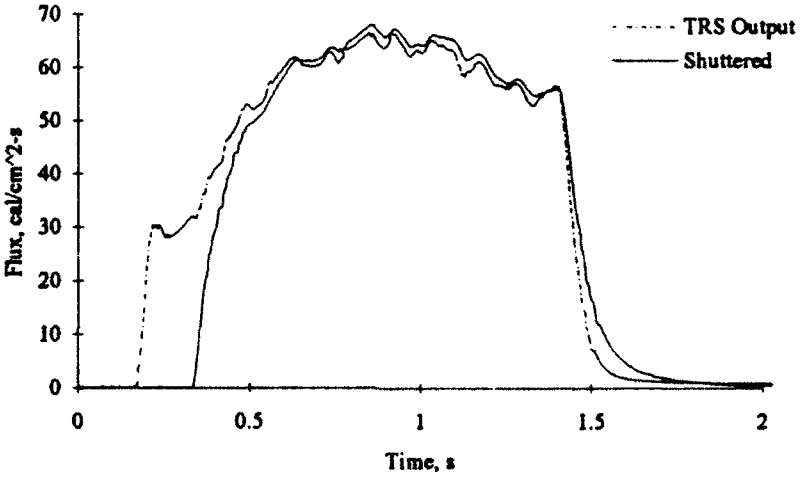

Figure 19. Response experiment data.

The two calorimetric data sets were compared using a data analysis program (DSP Development Corporation 1991). The shuttered set data were divided by the fully exposed set which yielded an exponential rise-time curve. Several curves of the response equation ($1-e^{-t/C_t}$) were created to be compared to the rise-time curve. The best fit of C_t was used to generate the corrected flux profile in Figure 17.

The response time would not affect the fluence data since the net difference of the measured and corrected fluence diminishes with time. The most profound effect is when the TRS output has to fall within specific performance requirements. If the TRS were to perform as prescribed, the sensor must respond at least five times faster. The rise and fall times appeared to improve with the correction. The standard deviation (Baumeister, Avallone, and Baumeister 1978), calculated as

Average: $$\bar{x} = \frac{\sum_{1}^{n} x_i}{n} ;$$

Standard Deviation: $$\sigma_D = \left[\frac{\sum_{1}^{n} (x_i - \bar{x})^2}{n-1} \right]^{1/2} ,$$

would result in σ_D well over 10% of the average flux. Further studies of the calorimeter response times need to be pursued to determine if the TRS would meet the parameters established and be ready to be introduced into the probative tube.

3.6.2 Data Recording.

The new data acquisition system was a product by OPTIM Electronics, Germantown, MD. It is a MEGADAC 2200C. This small system was controlled by a PC (the same one communicating with the controller and the TRS) and could record up to 126 channels of data.

The system operated sequentially, sampling the data from each channel in a stacked fashion. The data were stored digitally in the MEGADAC 2200C and retrieved by the PC when convenient. Figure 20 shows the schematic setup of the controller and data acquisition system and the way they were linked together through the PC.

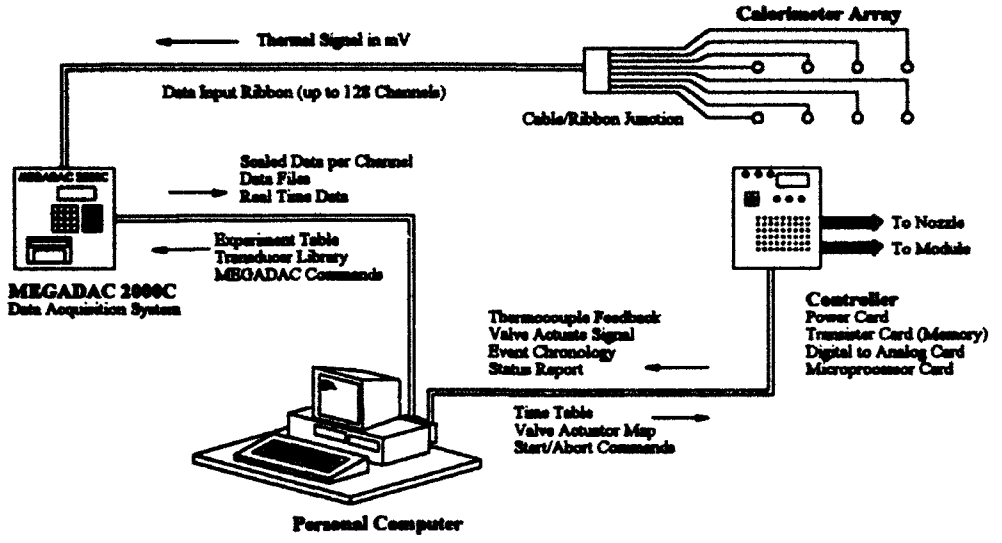

Figure 20. Controller and MEGADAC.

PC programming of the MEGADAC was accomplished through a custom-written program (Muller 1991). The program had a library containing all relevant information for each calorimeter used and produced data sets for each channel specifically tailored for ARL use. The program could be used to generate an "Experiment Table." This table would contain all pertinent facts such as experiment date, title, transducer type, sensitivity, location, triggering levels, sample rate, test duration, and other information. The tables are easily changed and are printed to maintain a permanent record. The turn around time for test results was reduced significantly. The data are already in digitized format so any analysis can be immediately started from the PC.

3.7 Aluminum Tank Pressure and Fluidization.

After the TRS was modified by adding the larger combustion chamber, the ball divert valve, and the new control system, TRS testing began. As evident from the TRS records, there was a distinct 6-Hz oscillation in the output, as seen in Figure 12. The amplitude was modulated to about 75% of the mean output, which was unacceptable. Presumably, the modulation was caused by a fluctuation in the aluminum powder mass flow rate from the aluminum tank. This mass flow fluctuation shows up in the thermal output as the oxygen-aluminum combustion process shifted between rich and lean mixtures.

The pressure and aeration system for the aluminum tank was suspected to be the cause of the problem. The system used a single pressure regulator. The regulated nitrogen gas traveled to a T-fitting. One end, with low volumetric flow, went into the tank to agitate the aluminum powder. This line was called the "fluidizer." Fluidization was necessary to make the aluminum flow like a liquid. The other end, of high volumetric flow, passed a check valve with a crack limit pressure of 90 psi, or pressure required to open the valve in the flow

direction, before entering the tank. This was termed the "driver." The driver was needed to pressurize the tank above the static pressure of the high-speed nitrogen line so the aluminum could be "driven" into the high-speed nitrogen from the tank.

To enhance the fluidization, the check valve was used to limit the pressure into the driver, allowing the fluidizer to remain at a higher pressure. The check valve was installed in line with the driver after the T-fitting. This prevented flow into the high volumetric flow line until the differential pressure reached the valve crack limit. The check valve would open, allowing the driver gas to enter the tank. The idea was higher pressure fluidizer gas would constantly flow, agitating the aluminum powder. Eventually the tank pressure dropped below a certain level due to being open to the high-speed line. The check valve would crack open and flow enough gas to make up for the flow deficiency of the fluidizer.

The check valve is designed to behave as an underdamped mass-spring system. When nitrogen flowed through the valve, it would cause the poppet and spring to chatter at approximately the same frequency as the thermal output oscillations. The only damping was coulomb friction and viscous effects on the poppet and spring. The valve also limited the volumetric flow.

The pressure regulator, T-fitting, and check valve were replaced with separate regulators for the fluidizer line and the driver line as shown by Figure 21. The fluidizer line remained low volumetrically, but was set at higher pressure. The driver line was high volumetrically, but remained set 68.9 kPa lower in pressure to establish the pressure gradient within the aluminum tank for powder agitation. This balance of pressure setting and volumetric flow difference provided stable pressurizing and fluidizing of the aluminum powder, eliminating the oscillating pneumatic effects.

Figure 22 demonstrates the success of these modifications in damping the flux oscillations. Not only was the depth of modulation decreased, but the average thermal output increased by a factor of two. The distinct 6-Hz oscillation was removed, but a small amplitude fluctuation of about 8 Hz to 10 Hz still existed. The fluctuation suggested that further modification of the TRS was needed.

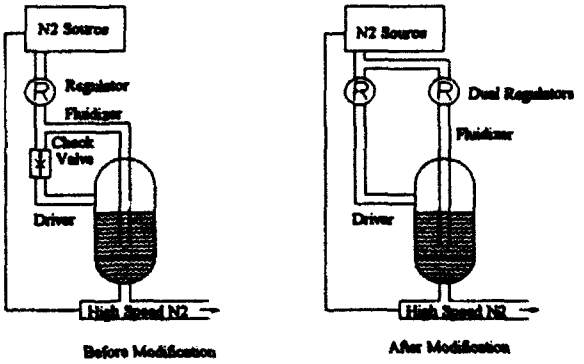

Figure 21. Modification of fluidizer/driver system.

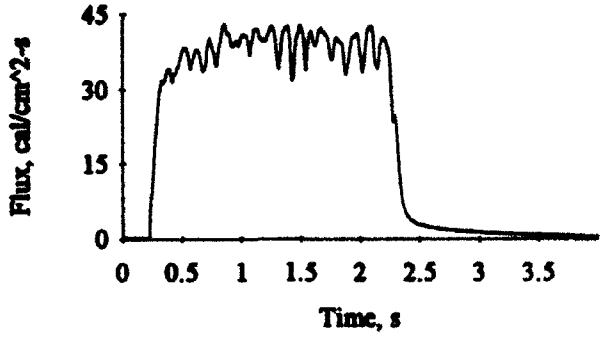

Figure 22. TRS flux record after modification of aeration/driver system.

The three-nozzle TRS system was provided with a flexible line for high-speed transport of the aluminum powder from the module to the nozzle 10 m distant. When the TRS was modified to a single nozzle configuration, as much of the original equipment as possible was used, and the flexible high-speed line was retained.

After the driver/fluidizer system was improved, there still persisted an 8-Hz to 10-Hz fluctuation in the thermal output, but of a much lesser magnitude than the former check-valve-induced oscillation. An engineering model of the aluminum tank pneumatics and the high-speed nitrogen line was developed. The model was an attempt to reproduce the oscillating mass flow.

The mathematical model of the pressurized aluminum tank revealed that the tank/high-speed line interface did *not* set up a resonance condition. If the pressure outside the exit of the tank were constant, then the mass flow rate of aluminum would be steady after an initial burst of powder. If the exit pressure of the aluminum powder tank were oscillatory, then the mass flow rate would be directly influenced. For a more detailed explanation of the mathematical model, see Appendix C.

The flexible high-speed line was investigated. It was found that some of the line was blocked. Aluminum powder had settled in some slight dips and curves and hardened. The line gave adequate passage when the aluminum was initially injected into the high-speed flow, but when the aluminum arrived at the blockage, the blockage would lower the mass flow until the initial aluminum mass passed through. Blockages, combined with the line's ability to expand in length, created pockets of aluminum powder concentration.

The flexline was eliminated, and a smooth-walled, rigid copper tube of equal inside diameter was installed. The result, as evident in Figure 23, is a relatively smooth and level thermal output with fast rise and fall times. By the changes described, ARL was able to create a TRS that has fairly precise output with a good approximation of a rectangular thermal pulse.

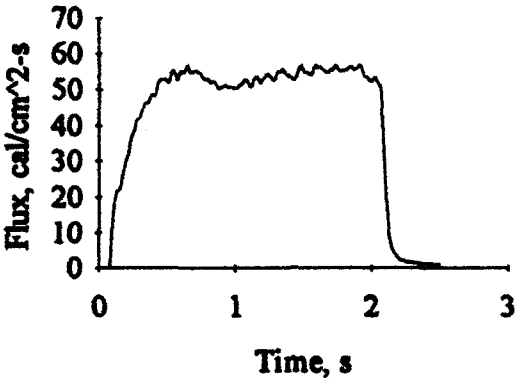

Figure 23. TRS flux record after modification of aluminum powder transport line.

3.8 Characterization Methods.

To evaluate the changes made to the TRS, a method to analyze the data was needed. Since the TRS output is nearly rectangular, four schemes that describe the output as a strictly rectangular pulse with defined amplitude and duration have been developed. The amplitude can be described as the average flux, and the duration is the time of thermal output at the defined average flux. These four schemes are the Full Width method, Full Width at Half Maximum method, Moments Matching method, and the presently preferred Fourier Averaging method (Loucks 1990).

3.8.1 Full Width Method.

The Full Width method defines the pulse width of the flux record as the time from the initiation of the TRS until the flux level has dropped below some minimum point close to the baseline. The amplitude is then determined by dividing the fluence, or the integrated flux record, by the pulse width. The beginning of a flux record is ordinarily well-defined, but the termination point is vague due to the hot cloud of residue still proximate to the target after shut-down. The still cooling aluminum oxide particles leave a decaying trail on the calorimeter data and prolongs the termination point. As seen in Figure 24, the determination of the pulse width usually leads to low amplitude levels, poorly characterizing the TRS data.

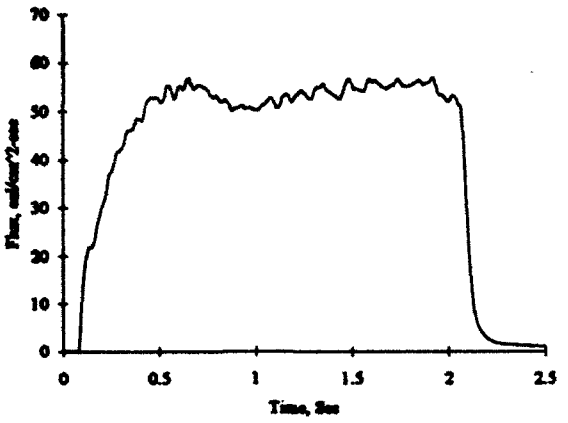

Figure 24. Comparisons between TRS data and Full Width method.

3.8.2 Full Width at Half Maximum Method.

This method is a corrected Full Width method. The Full Width method is modified by redefining the pulse width onset and termination points. As seen in Figure 25, these points are defined as where the flux record initially reaches more than one-half the maximum value and where the flux level drops below this value again. This method improves the ideal characterization because it is not prolonged by the residual burn-off.

Large variations in TRS output affect the repeatability of the TRS maximum. Determination of the half-maximum value changes between records. Because of the amount of this variation, crossover to below half-maximum could occur more than once. Multiple crossover below half-maximum presents a problem in some algorithms for establishing the parameters but can be overcome. A drawback to this method is that the exclusion of data outside the defined pulse length results in a low fluence calculation.

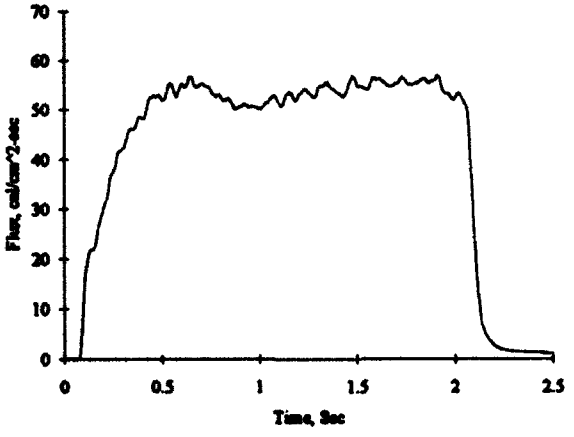

Figure 25. Comparisons between TRS data and Full Width at Half-Maximum method.

3.8.3 Moments Matching Method.

The Moments Matching Method can establish the parameters of the rectangular pulse from an arbitrary pulse in terms of its zeroth, first, and second moments. The equation is a time transformation of the data. The n'th moment is defined as

$$M_n = \int_{-\infty}^{+\infty} f(x)t^n dt.$$

The rectangle that is parameterized is the one which most closely matches the same moments. The amplitude A and the pulse width, pw, can be found centered about a point in time, t_c, from the following equations:

$$t_c = \frac{M_1}{M_0}, \qquad pw = 2\sqrt{3\left(\frac{M_2}{M_0} - t_c^{\,2}\right)}, \qquad A = \frac{M_0}{pw}.$$

The zeroth moment, M_0, is the fluence of the record, and determining pw is rigorous. The limitation of this characterization scheme is that pw is dependent on the second moment, M_2. The second moment is extremely sensitive to the range of data being observed. As the range of data points is increased, the instrumentation line noise will quickly affect the second moment value because of the t^2 term. The consequence is uncertainty regarding the calculated pulse width. The TRS data set must be carefully bounded to eliminate line noise outside what is considered pertinent data before analysis can be performed.

3.8.4 Fourier Averaging Method.

The Fourier Averaging Method (Loucks 1991[a]) is a reliable, rigorous method of characterizing a TRS data set, requiring no estimation or manual work. The idea is much the same as the Moments Matching method in that the data set is subjected to a transformation, then compared to a rectangular pulse subjected to the same process. The rectangular pulse that most closely matches that data defines the characterization parameters.

The Fourier transform of a time-dependent equation into the frequency domain is defined as such

$$G(f) = \int_{-\infty}^{+\infty} F(t)e^{-i2\pi ft}dt, \qquad G(f_0) = 0, \qquad pw = \frac{1}{f_o}.$$

The Fourier transform of a TRS data set will yield approximately the same transform results. By simply finding the first minimum point of the transformed record, the pulse width is established. The TRS data set is then fully characterized. The transform is relatively insensitive to the range of data used. Because of the insensitivity, data points can be bypassed or data sets decimated to increase the speed of characterization.

The Fourier transform will break into two parts, real and imaginary. The magnitude is the positive square root of the sum of the squares of the two parts. At 0 Hz, the energy density will be at a maximum. This is also the fluence of the TRS record. As the frequency increases, the resulting integration will decrease until eventually a minimum is reached. Since the magnitude is the positive square root of the sum of the squares, its value will never be negative. For a true rectangular pulse, this first minimum will be zero. Since TRS is a distortion of the rectangle, the minimum may not be zero, but the minimum is still clearly defined. The pulse width is defined as the reciprocal of the frequency where the magnitude of the transform is a minimum.

The minimum f_0 is unknown. Finding it is done by iteration since the solution requires a transformation from the time domain to the frequency domain. Fortunately, few iterations are required. The process can be made more rapid by first estimating the pulse width and concentrating the method in that area, but that is not necessary. The result is a method of characterizing the TRS thermal pulse without any estimations or manual work. The technique is rigorous and the result repeatable with precision.

3.9 TRS Analysis Program.

A TRS data reduction and analysis program called DANTE (Loucks 1991[b]) was written and placed on the same PC as the TRS controller and the data acquisition system to expedite the process of data analysis. Also with the ability of the MEGADAC 2200C to record several channels, a quick method to reduce, analyze, and review the TRS data on-site was needed.

All four characterization methods are used in DANTE. Each TRS calorimeter record is clipped of baseline data and run through the four characterization schemes. Each record is run through a statistical subroutine, which calculates an average flux, standard deviation, and nominal deviation.

For thermal mapping, the calorimetric data was also compared to a calorimeter placed in the same spatial reference point, called the standard, resulting in a normalized output. A resulting data record is shown in Figure 26. The data array produced from each calorimeter channel was divided by the same time-array element from the standard data set. This resulted in a "Percent" normalized result.

$$P_n\% = \frac{F_{data}(t_n)}{F_{stnd}(t_n)} 100\% .$$

The standard varies between burns. The data are more representative of the test series if a particular TRS burn were to deteriorate or exceed its average flux. Also, the normalized values could be easily adjusted to reflect any deviation of the reference to the average output of the TRS.

The result of DANTE is an information set for each channel. The development of DANTE has been very useful in finding and eliminating complications with the TRS output, performing tests for other projects and doing thermal mapping (Loucks 1991[a]).

The Analysis Sheet information provided input for a database for comparisons against other data sets of the same test. Each calorimeter was compared against the standard and other events. The normalizing was to evaluate the thermal radiation incident to an array member calorimeter relative to the standard. When the array setup was altered, the standard would reflect the normalized output when making comparisons. The first part of the sheet is TRS event identification and calorimeter data (location, channel). The ideal parameterization compared the four methods. The statistical analysis provided a way to measure the performance. The standard deviation and nominal deviation gave a measure of the amount of variation in the output during the steady-state phase. The normalized comparisons are the output divided by the standard.

TEST: Total Aluminum
SHOT: TRS-4-92
STATION: -60/-10/72
BEGINNING TIME: 0 sec
TIME INTERVAL: .004 sec
ARRAY SIZE: 2125 data points
TIME OF ARRIVAL: 3.362023E-03 sec
PEAK LEVEL: 107.1847 cal/cm^2-sec

IDEAL PARAMETERIZATION

METHOD	FLUENCE cal/cm^2	PULSE WIDTH sec	AVERAGE FLUX Cal/cm^2-sec
FULL WIDTH	426.281	6.068	70.74506
FULL WIDTH HALF MAX	401.9088	5.272	76.23461
MOMENTS MATCHING	429.281	5.618311	76.40749
FOURIER AVERAGING	429.2989	5.535471	77.55418

STATISTICAL ANALYSIS

MEAN = 72.6503 Cal/cm^2-sec
STANDARD DEVIATION = 18.45188 Cal/cm^2-sec
NOMINAL DEVIATION = 25.39822 %
TIME RANGE = 5.72 sec.
STATISTICAL CLIP STARTED AT .888 sec AND ENDED AT 6.608 sec

NORMALIZED COMPARISONS

COMPARISON AGAINST TRS-4-92 -60/-10/72
NORMAL MEAN = 100.0699 %
NORMAL STANDARD DEVIATION = 6.992616E-02 %
TIME RANGE = 5.724 SEC.
NORMALIZED CLIP STARTED AT .856 sec AND ENDED AT 6.58 sec

Figure 26. DANTE analysis sheet information.

4. SAFETY

The original TRS was not very safe to operate—the technology and mechanisms were untried, and the materials were considered hazardous. After the failure of the three nozzle source, the ARL program stipulated that the TRS must be safe to operate. An SOP was needed, and it had to consider the TRS's effects on personnel and the environment.

4.1 Personnel Impact.

Personnel operating the TRS must be protected from accidental thermal radiation, flames, cryogenics, electrical current, and aluminum powder. An SOP was written based on knowledge gained by experiments. Individuals also received proper clothing and training in the materials they were handling.

There are three substances used that require a Material Safety Data Sheet (MSDS). They are aluminum powder, LOX, and liquid nitrogen (LN2). All three substances are relatively harmless to the personnel except in special conditions. Careless handling of the cryogenic liquids could result in freezing injuries. Additionally, two individuals are needed for LN2 handling. One technician handles the equipment while the other observes the nitrogen transfer process from a distance. This precaution is taken in case the operator is accidentally overcome by an abundance of nitrogen, which could possibly displace oxygen for breathing.

The aluminum powder can present some hazard to the individual handling it. It is a combustible material. The handler must take care not to allow flames or sparks in his vicinity. Proper grounding must be ensured. A respirator and face shield is required. Exposure to high concentrations of aluminum powder can cause eye and respiratory system irritation (Reynolds Metals Company 1988). There are no known carcinogenic or reproductive effects.

4.2 Environmental Impact.

The TRS produces aluminum oxide and heat. The waste recovery bin catches at least 99% of the unused aluminum powder. The powder is recycled with some loss when transferring from the waste recovery bin to the aluminum powder tank or storage container. The wasted LOX and LN2 go back into the atmosphere. The aluminum oxide powder produced from the burn falls back to the ground and is dispersed onto the soil.

The area within a 30-m radius of the TRS is considered the "buffer" area, as seen in Figure 27. Any severe effects are realized within a 5-m radius, the "danger" area. Special care is needed when there is a target present. The thermal radiation effects on some coatings can cause chemical changes. Some of these coatings can become carcinogenic or poisonous. The toxic materials must be contained and disposed of properly.

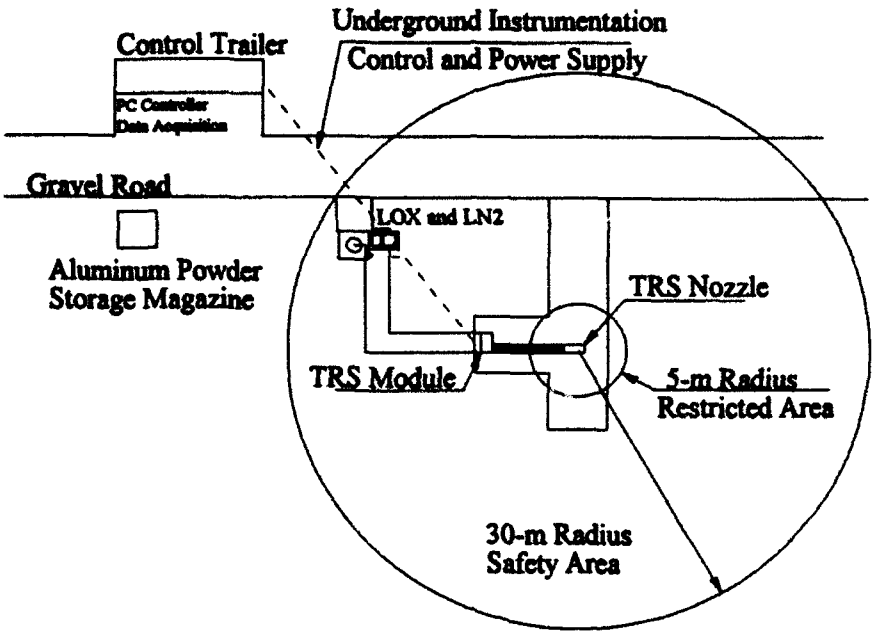

Figure 27. TRS facility layout.

4.3 Fire Hazards.

At present, the greatest danger is that some of the larger condensed particles of aluminum oxide are still above the ignition temperature of the material on which they fall. The danger is when these particles land in flammable areas or material (e.g., grassy areas, wood, or tar paper). The SOP dictates that no TRS operation will be conducted near any flammable materials. To ensure that hot particles do not get carried by wind outside the danger radius, the TRS is never fired in winds higher than 5 m/s.

The module is well within the 30-m buffer radius but is well protected from the TRS effects. The aluminum powder is contained in a heavy steel, airtight tank that is pressurized by nitrogen gas. The hydrogen and oxygen gas bottles are equipped with explosion-proof valves and are themselves immune to any hot particles. The LOX container is well-insulated and has a steel covering. The controller is enclosed in a steel container and is sealed before each test as directed by the SOP.

Four different fire extinguishers are available during a test. Two of these are class A and B extinguishers. One class C dry chemical extinguisher is available for fires involving energized electrical equipment, and a class D (Metalex) is available for any fires directly involving the aluminum powder (National Fire Protection Agency 1969). Sand is also available to contain aluminum powder fires and is the recommended method of fighting a metal dust fire (Aluminum Association 1985).

It is important to understand the use of the different extinguishers. By the MSDS for aluminum powder, the A-B-C extinguishers are not for use against the aluminum powder in the event of a fire. Pressurized systems

that could stir or react with burning aluminum will spread the aluminum powder. The agitation could cause the aluminum powder to form a cloud, increasing the oxygen-to-fuel ratio to dangerous levels. The sand is used to build a ring dam around the burning aluminum to contain the flames. The class D extinguisher, when released, sinks down onto the burning powder and smothers the fire.

The likeliest means of accidental ignition of aluminum powder is generation of a static electrical spark while the aluminum powder is being transferred. To ensure this does not happen, the TRS and accessories are grounded. The aluminum powder is stored in a vented, dry, and grounded shed 45 m from the TRS. The shed is made of wood, but the floor is covered with a wire mesh that is attached to a buried 1-m-long copper grounding rod. All the equipment used to handle the aluminum powder is nonsparking, conductive material. The TRS module is also connected to a 1-m copper grounding rod. A detachable grounding strap is attached to the TRS module and is clipped to the aluminum container during loading of aluminum powder into the aluminum powder tank. The grounding also helps prevent accidental ignition by lightning strikes.

5. SUMMARY

The performance guidelines for the ARL TRS Program have not yet been met. A repeatable, consistent, and uniform radiant field that can be inserted into the 2.44-m probative tube is not yet a realization. The modifications of the formerly damaged unit has resulted in a unit that was state-of-the-art. The rise and fall times of the flux record are no more than 100 ms and are probably better. The average variation during maximum thermal output is believed not to exceed 10%. Currently, fluence is predictable to within ±2%. More work needs to be performed to learn of the possible deficiencies of the calorimeter.

The addition of the large combustion chamber, three-way ball valve, and changes in the aluminum fluidization and transport were the most significant mechanical improvements to the TRS. Changing the control and data acquisition systems were the additional measures necessary for operation. The computer simulation of the aluminum pressure vessel was the beginning of modeling the entire system. The experiments resulted in learning that the TRS flame cannot be spread as predicted. The aluminum powder loses too much energy before it is past 1 m above the combustion chamber. There is a need to develop an advanced TRS that incorporates all lessons learned from this effort.

Three years of experimentation have provided experience in safely handling aluminum powder, cryogenics, and targets. An SOP to ensure the safety of personnel and protection of the environment has worked very well. The facility created for this type of experimentation has enabled ARL to continue this type of work. It is feasible to design improved TRS systems.

6. REFERENCES

Aluminum Association, Inc. "Recommendations for Storage and Handling of Aluminum Powders and Paste." TR-2, Washington, DC, July 1985.

Baumeister, T., E. A. Avallone, and T. Baumeister III. Marks' Standard Handbook for Mechanical Engineers. Eighth Edition, New York: McGraw-Hill Book Company, 1978.

DSP Development Corporation. DADiSP Version 3.0. Cambridge, MA, September 1991.

Loucks, R. B. "Thermal Radiation Simulator Characterization Methods for the Rectangular Pulse." BRL-TR-3148, U.S. Army Ballistic Research Laboratory, Aberdeen Proving Ground, MD, September 1990.

Loucks, R. B. "Optimization and Modification of a Thin Flame Thermal Radiation Source." Paper presented at the 12th International Symposium on Military Applications of Blast Simulation, Perpignon, France, September 1991[a].

Loucks, R. B. DANTE.BAS Version 1.3, U.S. Army Ballistic Research Laboratory, Aberdeen Proving Ground, MD, March 1991[b].

Loucks, R. B. "The Effect of Transducer Response Rate on Thermal Radiation Data." Paper presented at the 13th International Symposium on Military Applications of Blast Simulation, The Hague, The Netherlands, September 1993.

Mergnat, D. Conversation with author. Centre d'Etudes de Gramat, Gramat, France, 27 February 1990.

Muller, P. C. MEGA.BAS Version 1.0. U.S. Army Ballistic Research Laboratory, Aberdeen Proving Ground, MD, January 1991.

National Fire Protection Agency. Fire Protection Handbook. 13th Edition, Edited by G. H. Tryon and G. P. McKinnon, Boston, MA, 1969.

Polk, J. F. Conversation with author. U.S. Army Ballistic Research Laboratory, Aberdeen Proving Ground, MD, November 1991.

Rehmann, W. "Characterization of the Thermal Radiation Field Generated by a One-Nozzle Torch." BRL-TR-02529, U.S. Army Ballistic Research Laboratory, Aberdeen Proving Ground, MD, October 1983.

Reynolds Metals Company. "Material Safety Data Sheet." Form OSHA-174 for Grade 120 Aluminum Powder, Richmond, VA, November 1988.

Reynolds Metal Company. "Reynolds Aluminum Atomized Powder." Advertisement Number 730-1-7(5-189), Louisville, KY, 1990.

Van Wylen, G. J. and R. E. Sonntag. Fundamentals of Classical Thermodynamics. SI Version, Second Edition, New York: John Wiley and Sons, Inc., 1978.

APPENDIX A: TRS OPERATION CHECKLIST AND EXPERIMENT SHEET

Intentionally Left Blank

Operational Procedure for the "Thin Flame" TRS System.

1. Turn on the range warning lights and put safety barricades and warning signs in place.

2. Assure that fire extinguishers are charged and available.

3. Set safety relay switch in blockhouse to safe.

4. Install panel control key in controller at service module.

5. Check LOX and Al supply levels in service module tanks.

6. Check that the Al supply tank cap is securely installed and that the nozzle plug is removed.

7. Open the three nitrogen storage tank manual valves.

8. Clear the area of nonessential personnel and confirm that the panel control switch on the service module controller is off.

9. Turn on the TRS power supply in the blockhouse and place the safety relay switch in the operate position.

10. Adjust the N2 pressure regulators located on the service module to the output pressures listed on the operational checklist.

11. Place the panel control switch on the service module controller in the panel control position and the controller mode switch in the device test position.

12. Check the actuator operation of the functioning of the valves listed on the operational checklist.

13. After the valve actuators and valves have been functioned, record the N2 pressure regulator output pressures on the operational checklist.

14. Verify the operation of the TRS ignition system by performing the following steps. Open the O2 and H2 supply cylinders and check the supply tank pressures. Set the O2 and H2 regulator output pressures to the values listed on the operational checklist. Place the panel control switch on the controller to the panel control position and the controller mode switch in the device test position. Place controller in the ignition sequence mode and press the start switch to initiate igniters. After stable ignition operation is confirmed, press the stop switch to terminate the ignition sequence.

15. Place the panel control switch on the service module controller in the off position and the safety relay switch in the safe position.

16. Check the N2, O2, and H2 gas supply levels and the LOX and Al supply levels at the service module.

17. Close the N2, O2, and H2 gas supply valves.

18. With the safety relay switch in the safe position, place the panel control switch on the service module controller in the panel control position and the controller mode switch in the time set position. Check and/or set the controller function times as listed on the operational checklist.

19. Confirm that the safety relay switch is in the safe position and place the panel control switch on the service module controller in the remote position.

20. Load the control program (brlop.bas) into the control computer in the blockhouse and run the control program. Initiate test start from the blockhouse computer and verify the start of the service module controller. After verifying the service module controller start, abort the test from the blockhouse computer.

21. Place the panel control switch on the service module controller in the off position and confirm that the blockhouse personnel are ready to conduct the test.

22. Open the N2, O2, and H2 supply tank valves. Record the N2, O2, and H2 supply tank pressures and the O2 and H2 regulator output pressures on the operational checklist.

23. Place the panel control switch on the service module controller in the remote position and secure the controller door.

24. Confirm that the area is clear of personnel and record the weather conditions on the operational checklist.

25. Sound the range warning siren.

26. Place the safety relay switch in the operate position and initiate a reset from the blockhouse computer.

27. Verify instrumentation recorders are on and initiate the test start from the blockhouse computer.

28. Following the test, confirm that the blockhouse computer has timed out and the clock has stopped at 74.9 s.

29. Initiate a reset from the blockhouse computer and confirm that the Al and LOX tanks have vented.

30. Record the test identification data on the operational checklist.

31. Place the safety relay switch in the safe position and proceed to the service module. Place the panel control switch on the service module controller in the off position.

32. Check the area for fires and extinguish as required.

33. Close the O2 and H2 supply tank valves.

34. Sound the all clear on the range warning siren.

35. Place the safety relay switch in the operate position, place the panel control switch on the service module controller in the panel control position, and place the controller mode switch in the device test position.

36. Verify the nozzle area is clear of personnel and initiate the high-speed N2 flow. Initiate the Al pulse start and verify that the Al delivery line is purged.

37. Press the controller stop switch.

38. Close the three N2 supply tank manual valves.

39. Place the panel control switch on the service module controller in the off position and remove the switch key. Place the safety relay switch in the safe position and turn off the TRS power supply.

40. Return the panel control switch key to the blockhouse and turn off the range warning lights.

41. Remove the safety barricades and warning signs.

42. Install the nozzle plug and secure the service module control panel, the service module, and the nozzle module.

Operational Procedures for the Trailer Mounted High Pressure Cryogenic Pump/Vaporizer.

NOTE: Cryogenic liquids will cause severe freeze burns on contact with skin. Protective clothing and equipment must be used when operating this system.

1. Position LN2 dewars and cryogenic pump/vaporizer unit near the TRS service module to be pressurized so that a clear and unobstructed path of movement is provided between the units.

2. Connect the 1/2-in stainless steel flexible hose between the LN2 dewar and the cryogenic pump.

3. Connect the 1/4-in high-pressure hose from the vaporizer outlet to the input of the service module nitrogen manifold.

4. Check tightness of the connections of the stainless steel hose from the cryogenic pump to the vaporizer.

5. Close the manual input valve on the service module nitrogen manifold.

6. Open the three manual valves on the individual nitrogen cylinders and note the pressure on the nitrogen supply gauge (this will be needed when nitrogen transfer between the cryogenic pump/vaporizer and the nitrogen supply cylinders takes place).

7. Close the cryogenic pump bleed valve.

8. Check that the flow/vent valve on the vaporizer outlet is in the vent position.

9. Open the outlet valve on the LN2 dewar 1/4 to 1/2 turn (a loud hissing should be heard from the vaporizer vent line).

10. Check all connections for liquid or pressure leaks and tighten if required.

11. Fully open outlet valve on the LN2 dewar. Frost should form on the 1/2-in stainless steel flexible hose and the head of the cryogenic pump. (Check for leaks around the pump head gasket and tighten head bolts if required. Head bolts should be tightened carefully and only enough to stop leaking. Do not overtighten.)

12. Press the start button on the pump control unit.

13. Open the cryogenic pump bleed valve two full turns.

14. Turn the flow/vent valve on the vaporizer outlet from vent to flow position (the sound of N2 venting from the vaporizer should stop, and venting should be heard from the pump bleed valve).

15. Slowly close the cryogenic pump bleed valve to about 1/4-turn open until pump is primed (a deep throbbing sound indicates the pump has primed). (N2 vapor and a small trickle of LN2 will be coming from the bleed valve. This is necessary to prevent vapor lock and loss of prime in the pump.)

16. Check the pressure gauge on the cryogenic pump control box. (The green indicator indicates the automatic preset cut-off pressure of the pump control, and the black indicator is the system output pressure.)

17. When the system output pressure equals the pressure in the nitrogen supply cylinders, open the nitrogen manifold valve to fill the supply cylinders. (Unless system output pressure and nitrogen supply pressure are equal when manifold valve is opened, blow back can occur, which can cause the cryogenic pump to lose prime or damage the system.)

18. When automatic preset cut-off pressure is reached (2100 psi at the pump), the pump will cut off:

a. close the three manual nitrogen supply cylinder valves;

b. close the manual nitrogen manifold valve;

c. turn the flow/vent valve on the vaporizer outlet from flow to vent;

d. push stop button on the pump control unit;

e. close the outlet valve on the LN2 dewar (venting will continue from the vaporizer vent line and the pump bleed valve until all pressure has been relieved).

Operational Procedures for the Transfer of Liquid Oxygen from Bulk Storage to the TRS.

NOTE: Cryogenic liquids will cause severe freeze burns on contact with skin. Protective clothing and equipment FREE OF PETROLEUM-BASED CONTAMINANTS must be used when operating this system.

1. Confirm that the safety relay control switch is off.

2. Erect safety barricades and warning signs.

3. Install the panel control key in the controller and confirm that the panel control switch is in the off position.

4. Check and record the LOX level in the bulk storage tank. A minimum of 12 in of LOX is required to fill the service module tank.

5. Clear the area around the bulk storage tank and the service module of nonessential personnel to a distance of 30 ft.

6. Turn on the range warning flasher lights.

7. Open the manual LOX fill valve on the service module LOX tank.

8. Close the LOX transfer line vent valve at the LOX bulk storage tank.

9. Open the LOX transfer line valve at the LOX bulk storage tank.

10. Open the LOX supply valve at the LOX bulk storage tank to initiate the flow of LOX to the service module tank.

11. Confirm that gas is flowing from the service module LOX tank vent line.

12. Continue the transfer of LOX until a thin stream of LOX is seen flowing from the service module LOX tank vent line.

13. Close the LOX supply valve at the LOX bulk storage tank.

14. Open the LOX transfer line vent valve at the LOX bulk storage tank.

15. Close the manual LOX fill valve on the service module LOX tank.

16. Check and record the LOX level remaining in the bulk storage tank.

17. Place the service module panel control switch in the panel control position and check and record the LOX level in the service module LOX tank.

18. Place the panel control switch in the off position and remove the switch key.

19. Turn off range warning flasher lights.

Operational Checklist for TRS Operation.

Operational Checklist for " Thin Flame " TRS System . . . . Page 1

1. RECORD test data: ** ____
   a. Test identification number ___/___/___
   b. Test date ___/___/___
   c. Time _____:_____
2. Range warning lights ON ____
3. Safety barricades & warning signs PLACED ____
4. Fire extinguishers AVAILABLE & PLACED ** ____
5. Compressor for water pressure ON ____
6. TRS power ON Check Voltage level 32 V ____
7. Safety relay switch SAFE ____
8. CHECK supply levels:
   a. LOX supply _____ % ____
   b. AL supply _____ inches from top ____
9. Al tank cap INSTALLED ____
10. Nozzle plug REMOVED ____
11. Area CLEAR of non-essential personnel ____
12. Power ON Panel, control key INSTALLED in controller ____
13. Panel control switch PANEL CONTROL ____
14. Controller mode TIME SET ____
15. SET/CHECK controller function times:
    a. Cycle start _____ sec ____
    b. Ignition sequence start _____ sec ____
    c. Quit ignition, O2 on _____ sec ____
    d. LOX tank pressurization _____ sec ____
    e. Al tank pressurization _____ sec ____
    f. Nozzle purge _____ sec ____
    g. Vent tanks, end run _____ sec ____
    h. no function _____ sec ____
    i. LOX flow on _____ sec ____
    j. LOX Divert _____ sec ____
    k. Device A _____ sec ____
    l. Stop LOX & HS N2 flow _____ sec ____
    m. HS N2 flow start _____ sec ____
    n. Device B _____ sec ____
    o. Aluminum flow start _____ sec ____
    p. Aluminum flow stop _____ sec ____
    q. Aluminum pulse start _____ sec ____
    r. Aluminum pulse stop _____ sec ____
16. Panel control switch REMOTE ____
17. LOAD & RUN brlopr.bas on control computer ____
18. Initiate test START from control computer ____
19. VERIFY controller start ____
20. ABORT test from control computer ____
21. Controller Mode DEVICE TEST ____
22. Panel control switch PANEL CONTROL ____
23. Safety Relay switch ON ____
24. OPEN N2 tank valves & CHECK pressure _____psi ____
25. Actuators regulator output pressure SET to _____ psi ____

26. CHECK operation of valves:
    a. LOX tank pressurization ____
    b. AL tank pressurization ____
    c. Nozzle Purge ____
    d. LOX flow ____
    e. LOX to Nozzle ____
    f. Device A ____
    g. High speed flow ____
    h. Al pulse start ____

27. VERIFY operation of TRS ignition system:
    a. OPEN O2 cylinder ** ____
    b. CHECK O2 supply/output pressure ____/____ psi ** ____
    c. OPEN H2 cylinder ** ____
    d. CHECK H2 supply/output pressure ____/____ psi ** ____
    e. Personnel CLEAR of nozzle area 30 ft minimum ** ____
    f. Controller mode IGNITION SEQUENCE & START ** ____
    g. CONFIRM stable ignition operation ** ____
    h. STOP to turn off ignitors ** ____

28. Regulator output pressures SET to listed pressures:
    a. LOX tank pressure _____ psi
    b. High speed nitrogen _____ psi ____
    c. Aluminum tank driver pressure _____ psi ____
    d. Aluminum tank fluidizer pressure _____ psi ____
    e. Nozzle purge _____ psi ____

29. Control Panel switch REMOTE ____
30. Control Panel SECURE ____
31. Area CLEAR ____
32. SOUND warning siren ** ____
33. Safety relay switch OPERATE ____
34. Blockhouse READY for test ____
35. Initiate RESET from control computer ____
36. Initiate test START from control computer ____
37. Recorder ON ** ____
38. RECORD weather conditions: ** ____
    a. Temperature _____ F
    b. Barometric pressure _____ in Hg
    c. Wind direction _____
    d. Wind speed _____ mph

39. CONFIRM controller clock STOPPED at 74.9 sec ____
40. Confirm LOX and AL tank vents OPEN ____
41. Safety relay switch SAFE ____
42. CHECK area for fires/EXTINGUISH if required ** ____
43. Panel control switch OFF ____
44. EXTRACT Panel control key from controller ____
45. H2 cylinder valve CLOSED ** ____
46. O2 cylinder valve CLOSED ** ____
47. CLOSE Nitrogen tank valves ____
48. TURN DOWN all output regulators and let bleed ____
49. SOUND warning siren all clear ** ____

NOTE: ** Delete items when conducting "Cold Flow" Test

Experiment Data Sheet

DANTES Thermal Radiation Simulator
Experiment Data Sheet

Pre-Event Data

EVENT ID NUMBER TRS- -9 DATE / /
WEATHER
TEMPERATURE F HUMIDITY % BAROMETRIC in Hg
WIND DIRECTION: N NE E SE S SW W NW WIND SPEED mph
PRELIMINARY COMMENTS

INITIAL SETTINGS

ALUMINUM TANK DRIVER	psi	ALUMINUM TANK FLUIDIZER	psi
NOZZLE PURGE	psi	ACTUATOR PRESSURE	psi
LIQUID OXYGEN TANK	psi	OXYGEN PRESSURE	psi
HIGH-SPEED NITROGEN	psi	HYDROGEN PRESSURE	psi
ALUMINUM FLOW TIME	sec	ALUMINUM PULSE TIME	sec

ALUMINUM WEIGHT DATA

DISPENSER WEIGHT lbs

Distribution:

lbs	lbs	lbs
lbs	lbs	lbs
lbs	lbs	lbs
lbs	lbs	lbs

TOTAL WEIGHT lbs - ( )*DP = NET WEIGHT lbs

CALORIMETER LOCATION

ID#	LOCATION	ID#	LOCATION	ID#	LOCATION
	/ /		/ /		/ /
	/ /		/ /		/ /
	/ /		/ /		/ /
	/ /		/ /		/ /
	/ /		/ /		/ /
	/ /		/ /		/ /
	/ /		/ /		/ /
	/ /		/ /		/ /
	/ /		/ /		/ /
	/ /		/ /		/ /

Post-Event Data

ALUMINUM LEVEL

ALUMINUM TANK INITIAL LEVEL FROM TOP_____in
ALUMINUM TANK FINAL LEVEL FROM TOP_____in
NET CHANGE IN LEVEL_____in

CALORIMETER RESULTS

CALORIMETER ID	PEAK FLUX	FLUENCE	MEAN FLUX
1			
2			
3			
4			
5			
6			
7			
8			
9			
10			
11			
12			
13			
14			
15			
16			
17			
18			
19			
20			
21			
22			
23			
24			
25			
26			
27			
28			
29			
30			

COMMENTS_____

Intentionally Left Blank

APPENDIX B: METHOD FOR CORRECTING CALORIMETRIC DATA

Intentionally Left Blank

The work in this appendix is an expansion of the contribution of Dr. John Polk.

The Gardon-type gauge, depicted in the text in Figure 17, is not an instantaneous measurement device. It has a response unique to its physical design. The supplier of the gauge used at ARL has reported the response rate in very specific terms. If the gauge were subjected to a step input, the result is an exponential rise of $(1-e^{-t/C_t})$. The response specification is that 68.2% of the input would be registered in the output by a certain time. This time is the first time constant, C_t. By knowing the time constant, one can "correct" the output from the Gardon gauge.

Given the following definitions:

V_m is voltage produced from calorimeter

C_{TC} is proportionality constant

T_D is the diaphragm center temperature

T_B is the diaphragm edge temperature and is assumed constant with time

C_{VF} is a proportionality constant converting voltage to flux

C_{VT} is the product $C_{VF}C_{TC}$

F_m is the measured flux in cal/cm^2

F_i is the incident flux in cal/cm^2

C_p is the specific heat of the material

m is the diaphragm mass

The output of the Gardon-type gauge can be written as:

$$V_m = C_{TC}(T_D - T_B). \qquad \text{B-1}$$

The measured flux can then be written using equation B-1:

$$F_m = C_{VF}V_m = C_{VT}[T_D - T_B] \quad . \qquad \text{B-2}$$

For a transient analysis, the change in internal energy of the sensing element can be written as:

$$\Delta E = C_p m(T_D - T_B) \, . \qquad \text{B-3}$$

The rate of change in the internal energy can be written as:

$$\frac{d\Delta E}{dt} = \frac{d(C_p m T_D)}{dt} \, . \qquad \text{B-4}$$

The rate of change of the internal energy of the diaphragm is assumed to equal the net exchange of energy between the radiant flux into the surface and the energy conducted away at the edge. That could be written as:

$$\frac{d\Delta E}{dt} = F_i - F_m = F_i - C_{VT}(T_D - T_B) \, . \qquad \text{B-5}$$

This sets up a differential equation:

$$\frac{dT_D}{dt} = \frac{F_i + C_{VT}T_B}{C_p m} - \frac{C_{VT}T_D}{C_p m} \quad \text{B-6}$$

The solution of this differential equation can be found several ways. The method of using an integration factor is used. In general for any differential equation in the form:

$$\frac{dy}{dx} + yP(x) = G(x) \quad , \quad \text{B-7}$$

the solution can be expressed as:

$$y = \frac{1}{\mu(x)}\left[\int_0^x \mu(s)G(s)ds + C_{const}\right] \quad , \quad \text{B-8}$$

where

$$\mu(x) = \exp\left[\int_0^x P(s)ds\right] \quad . \quad \text{B-9}$$

By substituting the terms of equation B-6 into equation B-8 and equation B-9, and simplification, the result is a solution for T_D in the form of F_m and F_i. This solution is:

$$F_i = F_m + \frac{C_p m}{C_{VT}}\left(\frac{dF_m}{dt}\right) \quad . \quad \text{B-10}$$

As it turns out, the constant $\frac{C_p m}{C_{VT}}$ is equivalent to time constant C_t in the response rate equation, $(1-e^{-t/C_t})$.

APPENDIX C: PROCESS OF SIMULATION OF DRIVER/AERATION MODEL

Intentionally Left Blank

C.1 Aluminum Vessel Model.

An original mathematical model of the aluminum containment vessel was constructed to simulate the interaction of pneumatic forces with the dynamic forces of the powdered aluminum. The first approximation of the vessel dynamics did not take into account the possibility of variation in back pressure. It was assumed that the aluminum would be discharged into a constant pressure environment. The vessel included an aeration system to "fluff" the aluminum powder during an event so the aluminum would behave as a liquid.

As illustrated in Figure C-1, the dynamic model was represented by the following equations.

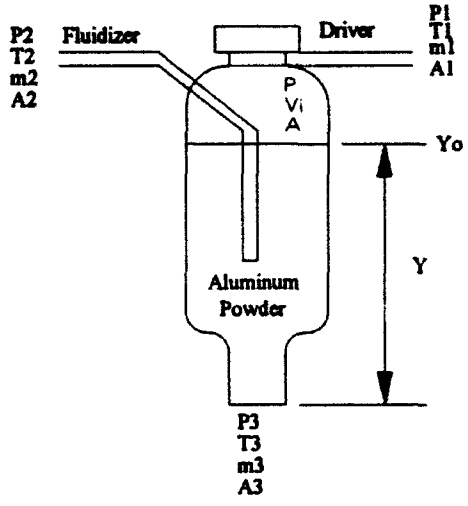

Figure C-1. Aluminum containment vessel.

Bernoulli's Equation,

$$\frac{P - P_g}{\rho_{AL}} + \frac{V^2}{2} + g_r y = \frac{P_3 - P_g}{\rho_{AL}} + \frac{V_3^2}{2} + g_r y_3 , \qquad \text{(C-1)}$$

By continuity and conservation of mass,

$$\dot{m} = \rho_{AL} V A = \rho_{AL} V_3 A_3 ,$$

and

$$V_3 = V \frac{A}{A_3} . \qquad \text{(C-2)}$$

Noting the velocity of the fluid level, V = dy /dt, denoted as y' so that

$$y_3' = y' \frac{A}{A_3}. \tag{C-3}$$

Collecting terms to one side and simplifying, a differential equation results in the form of

$$y' = \pm \sqrt{\frac{2\dfrac{P - P_3}{\rho_{AL}} + g_r y}{\left(\dfrac{A}{A_3}\right)^2 - 1}}. \tag{C-4}$$

This basic equation describes the pressure driving the aluminum through the bottom opening by the lowering of the aluminum level y from y_0. The assumptions are that the pressure P has an initial value, and there is no make-up air to maintain pressure.

The aluminum vessel in fact has two feed lines of nitrogen under pressure. The line pressure and flow volume are controlled by preset regulators. As pressure drops in the tank void, the make-up feed pressure increases, repressurizing the void to drive the aluminum powder. By using ideal gas laws and isentropic relationships, we are able to model the events occurring within the tank. Study of these events is easily done by observance in some small increment of time, Δt. This gives rise to the following modification of the ideal gas law:

$$P_o + dP = \frac{R(m_o + dm)(T_o + dT)}{V_o + dV}.$$

By using the following,

$$k = \frac{C_p}{C_v} \quad \text{(ratio of specific heats)},$$

and

$$R = C_p - C_v \quad \text{(gas constant)},$$

the result is the following relations

$$T_o + dT = T_o \left[\frac{P_o + dP}{P_o}\right]^{\frac{k-1}{k}},$$

and

$$V_o + dV = V_o + A(y_o - y).$$

Substitution yields a new pressure incremented by Δt,

$$P_o + dP = \left[\frac{RT_o(m_o + dm)}{\left[V_o + A(y_o - y)\right] P_o^{\frac{k-1}{k}}} \right]^k . \qquad \text{(C-5)}$$

The value of dm is the amount of mass being introduced back into the volume for repressurization during time increment Δt. Keeping in mind there are several inputs of gas into the volume,

$$\dot{m}_t = \sum_n \dot{m}_n ,$$

$$\dot{m}_n = A_n \rho_n \left(\frac{P}{P_n} \right)^{\frac{1}{k}} \sqrt{\frac{2kRT_n}{k-1} \left[1 - \left(\frac{P}{P_n} \right)^{\frac{k-1}{k}} \right]} . \qquad \text{(C-6)}$$

Simplifying and multiplying $\dot{m}$ by Δt results in

$$m = m_o + \sum_n \alpha_n \left[P^{\frac{1}{k}} \left(P_n^{\frac{k-1}{k}} P^{\frac{1}{k}} - P \right) \right] \Delta t , \qquad \text{(C-7)}$$

where

$$\alpha_n = A_n \sqrt{\frac{2kP_n^{\frac{k-1}{k}}}{RT_n(k-1)}} .$$

Substitution of equation C-6 into C-5 gives

$$P^+ = \left[\frac{RT_o \left(m_o + \sum_n \alpha_n \left[P^{\frac{1}{k}} \left(P^{\frac{k-1}{k}} P^{\frac{1}{k}} - P \right) \right] \Delta t \right)}{\left[V_o + A(y_o - y) \right] P_o^{\frac{k-1}{k}}} \right]^k . \qquad \text{(C-8)}$$

C.2 Descending Disk Method.

The resultant equations were run on a PC using FORTRAN. The results were a smooth, nonoscillatory mass flow of aluminum. The initial part of the simulation was extremely transient. Much like a damped system, the transients gave way to steady values of pressure and mass flow. The parameters were changed to extreme values in an attempt to stimulate instabilities. The one parameter that had significant effect was the outlet pressure, P_3. Varying the pressure had a commanding effect on the mass flow rate out of the aluminum tank.

To determine if the outlet pressure was affected by the current hardware configuration, a second model employing a technique called the "Descending Disk" (Loucks 1991)[1] method was used . As seen in Figure C-2, the mass out of the tank into the transport line is viewed as a solid disk of material. As the disk enters the transport line control volume during some time increment Δt, the transport pressure, P_3, is affected.

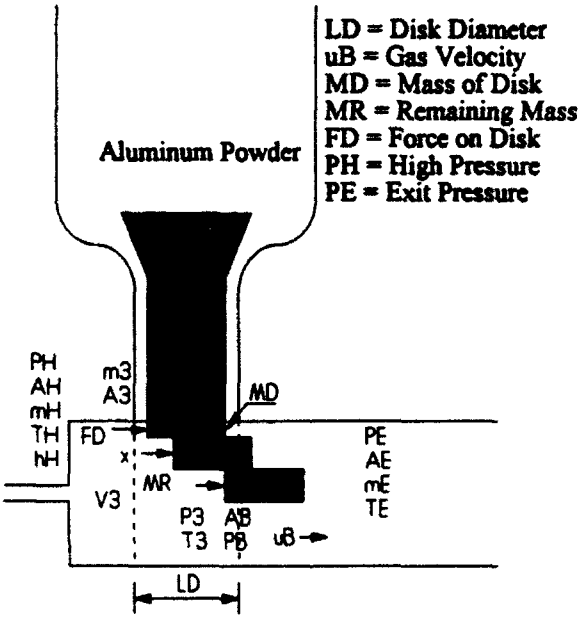

Figure C-2. "Descending disk" configuration.

Initially, as the disk lowers into the control volume, A_B will become some fraction of A_E, reducing $\dot{m}_a$, the air bypassing the disk. This will increase P_3. Within the time step, the descendant mass, M_D, will be accelerated out of the control volume. Any mass remaining in the control volume after Dt will be added to the

[1]Loucks, R. B. " Dynamic Reponse Formulation for Pneumatically Driven Liquid in a Pressure Vessel. "Proceedings of the 1991 American Society of Mechanical Engineers International Computers in Engineering Conference and Exposition, Santa Clara, CA, vol 2, p. 43, August 1991.

future mass/disk. The following is used

$M_D = \dot{m}_3 Dt$ (disk mass),

$r_D = \frac{M_D}{A_B L_D}$ (disk density),

$b = \frac{r_D}{r_3}$ (density ratio),

$A_B = A_B(1-b)$ (bypass area),

$F_D = P_3 b A_B = M_D \ddot{x}$ (force moving disk downstream).

The distance the disk travels downstream is determined by integrating $\ddot{x}$;

$$\ddot{x} = \frac{P_3 \beta A_E}{M_D}$$

integrates incrementally into

$$x = \frac{P_3 \beta A_E (\Delta t)^2}{2 M_D}.$$

The mass remaining within the control volume is

$$M_R = M_D\left(\frac{L_D - x}{L_D}\right), \text{ (if } x \geq L_D, \text{ no mass remains)}.$$

The remaining mass is important. It determines the amount of blockage in the control volume for the evaluation of change in P_3. To further evaluate what P_3 is, the control volume is treated as a vessel with given entrance and exit pressures and mass flows during some increment of time, Δt, as depicted in Figure C-3.

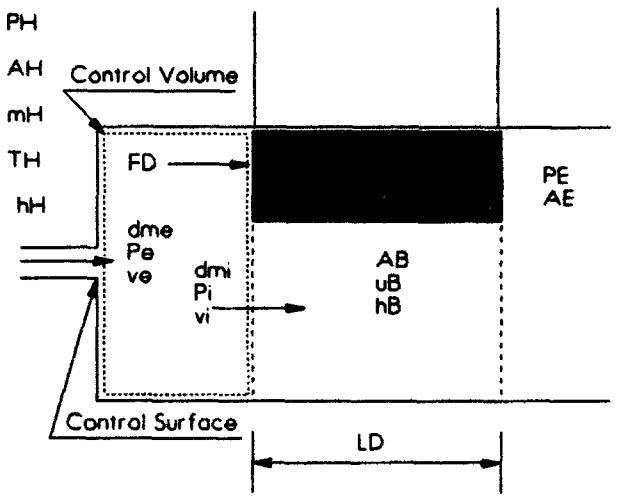

Figure C-3. Control volume during Δt.

To describe the change in internal energy of the control volume, we use the First Law of Thermodynamics (Van Wylen and Sonntag 1978)[1] :

$$\frac{dQ}{dt} = \frac{E_2 - E_1}{dt} + \frac{dW}{dt},$$

where the following are defined:

$E_1 = E_T + e_i dm_i,$

$E_2 = E_T + \Delta E + e_e dm_e,$

$dQ = 0,$ (adiabatic system),

$dW = dW_D + (P_e v_e dm_e - P_i v_i dm_i),$

$dW_D = \frac{F_D(x - L_D)}{\Delta t},$

By substitution and combination and using the following relations,

$$e + Pv = i + Pv + \frac{u^2}{2} + g_r z,$$

where e is described as the total specific energy of the working fluid The specific enthalpy is defined as $h = i + Pv$. The result is the following for the total net change in internal energy:

[1] Van Wylen, G. J. and R. E. Sonntag. Fundamentals of Classic Thermodynamics. SI Version, Second Edition, New York: John Wiley and Sons, Inc., 1978.

$$\Delta E = \left[h_H \dot{m}_H - \left(h_B + \frac{u_B^2}{2} \right) \dot{m}_B \right] \Delta t + \frac{F_D (L_D - x)}{\Delta t} \quad . \tag{C-9}$$

This equation describes the change of state of the working fluid, nitrogen, for the increment of time Dt. Several of the variables are yet to be defined. By use of the ideal gas law, and assuming the process is nearly isentropic and adiabatic, values for the unknowns can be found as follows. The mass flows of the inlet at H and the bypass at B are equated the same as equation C-6.

$$\dot{m}_H = A_H \rho_H \left(\frac{P_3}{P_H} \right)^{\frac{1}{k}} \sqrt{\frac{2kRT_H}{k-1} \left[1 - \left(\frac{P_3}{P_H} \right)^{\frac{k-1}{k}} \right]} \,,$$

$$\dot{m}_B = A_B \rho_B \left(\frac{P_3}{P_B} \right)^{\frac{1}{k}} \sqrt{\frac{2kRT_B}{k-1} \left[1 - \left(\frac{P_3}{P_B} \right)^{\frac{k-1}{k}} \right]} \,.$$

By use of the First Law

$$h_3 = \frac{u_B^2}{2} + h_B,$$

and

$$h_3 - h_B = \frac{u_B^2}{2} = C_p [T_3 - T_B].$$

By use of the isentropic relationship Pv^k = Constant,

$$\frac{T_3}{T_B} = \left(\frac{P_3}{P_B} \right)^{\frac{k-1}{k}} \,,$$

the kinetic energy term can be found to be

$$\frac{u_B^2}{2} = \frac{RT_3 k}{k-1} \left[1 - \left(\frac{P_3}{P_E} \right)^{\frac{k-1}{k}} \right],$$

The enthalpy of state B can be approximated by

$$h_B \approx C_p T_B.$$

Since the exit pressure for surface B is the inlet pressure for surface E,

$$P_B = P_E$$

then,

$$h_B = \frac{P_E k}{\rho_B (k-1)}.$$

The values for F_D are found from P_3 acting on A_E such that the work on the disk is expanded to

$$\frac{F_D(L_D - x)}{\Delta t} = \frac{P_3 \beta A_E L_D}{\Delta t} - \frac{(P_3 \beta A_E)^2 \Delta t}{2M_D}.$$

By substituting these values back into equation C-9, and knowing the value for h_H (found in gas tables), ΔE is fully determined.

We redefine the net change in energy of the control volume by the time increment. Previously ΔE was defined by the change in state of control surface. It is also defined by the change in state of the control volume itself over some time Δt. By use of the equations of state before and after Δt, using a constant volume analysis,

$$\Delta E = C_v (T_3^+ - T_3).$$

Again, using the Ideal Gas Law,

$$\Delta E = \frac{P_3^+ v_3^+ - P_3 v_3}{k-1},$$

where the specific volume (reciprocal of the density)

$$v_3^+ = \frac{V_3}{M_3^+}, \qquad v_3 = \frac{V_3}{M_3},$$

and

$$M_3^+ = M_3 + (\dot{m}_H - \dot{m}_B)\Delta t = M_3 + \Delta M.$$

By substitution and rearrangement, the predicted pressure P_3 is shown to be

$$P_3^+ = \left[\frac{\Delta E(k-1)}{V_3} + \frac{P_3}{M_3}\right](M_3 + \Delta M) . \qquad \text{(C-10)}$$

The results of P_3^+ can be inserted back into equation C-4 for determination of the pneumatic effects of the transport chamber at the foot of the aluminum tank. The entire process can occur and is advanced one time increment.

Assuming the model was not in error, and the output was believable, then the instabilities in the aluminum mass flow must be due to some other outside influence on this system. After some research of the hardware, it was found that the line transporting the aluminum powder was flexible and had several bends. These were hypothesized as to be the cause of the fluctuations, and a new straight, rigid pipe should replace the existing flex line.

A FORTRAN program was run on a PC to simulate the model. With given constants and initial values for variables, the program was able to simulate the mass flow of aluminum powder out of the aluminum powder tank, $\dot{m}_3$. The results of this simulation exhibited a steady mass flow rate. Attempts were made to cause the flow to oscillate. The oscillations were quickly damped and the flow stabilized. This led to the assumption that the source of the TRS output fluctuations was induced elsewhere.

It was found that the flexible transport line that carried the aluminum powder from the aluminum powder tank to the nozzle could be the source of a pressure undulation. A steady sinusoidal forcing function was applied at the pressure at the nitrogen pressurizer. The effect was to directly influence the mass flow rate. This indicated that the mass flow rate could be disrupted by an exterior influence. The flexible transport line was replaced by a rigid copper tube. The resultant TRS output demonstrated a sharp attenuation in the thermal output oscillations.

Intentionally Left Blank

APPENDIX D: MICROGRAPH DATA OF ALUMINUM POWDER

Intentionally Left Blank

The mounted stub with an aluminum powder sample for microscopic viewing consisted of two regions, as seen in Figure D-1. One part of the stub was painted with carbon adhesive and the remainder left untouched. A small sample of powder was shaken over the stub. After the adhesive dried, loose particles were shaken off and the entire mount was sputtered with a thin film of gold. The gold enhanced the topographic contrast and also improved the adhesion of the particles to the stub.

In the carbon adhesive areas, particles adhered in a dense heterogeneous array. This region, shown in Figure D-2, provides a sampling of the complete particle size but is probably biased toward larger particles. The low-magnification micrographs provided a general impression of the range of sizes present in the sample.

In the remaining region, Figures D-3 and D-4, particles of about 10-20 μm in size adhere to the mount by electrostatic attraction in a fairly uniform dispersion array. This region provided a better view of the finer components of the total distribution. Particles larger than about 20 μm did not appear since they will not adhere this way. However, it is considered that the total array is probably at least qualitatively representative of the particle distribution below about 20 μm.

The higher magnification micrographs in the nonadhesive region, Figures D-5 and D-6, provided an idea of the size distribution, shape, and general appearance of the particles. Higher magnifications of both regions show particle aspect and topography. In general, the fines are not strongly aggregated, but there is some tendency for the fines to be aggregated to the larger particles. The topography of the large particles show them to be primarily distinct entities rather than loose aggregations of smaller particles.

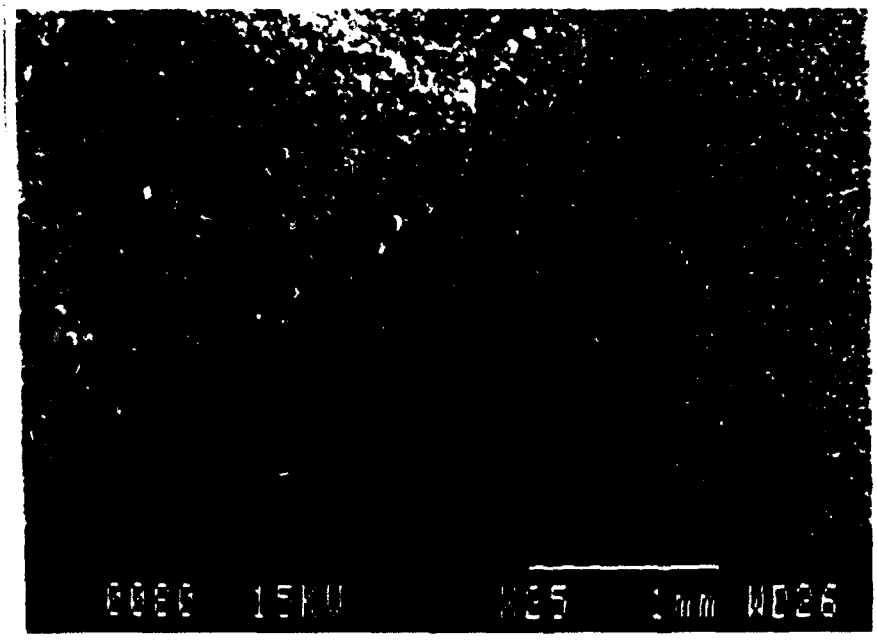

Figure D-1. Grade 120 aluminum powder mount at 25X.

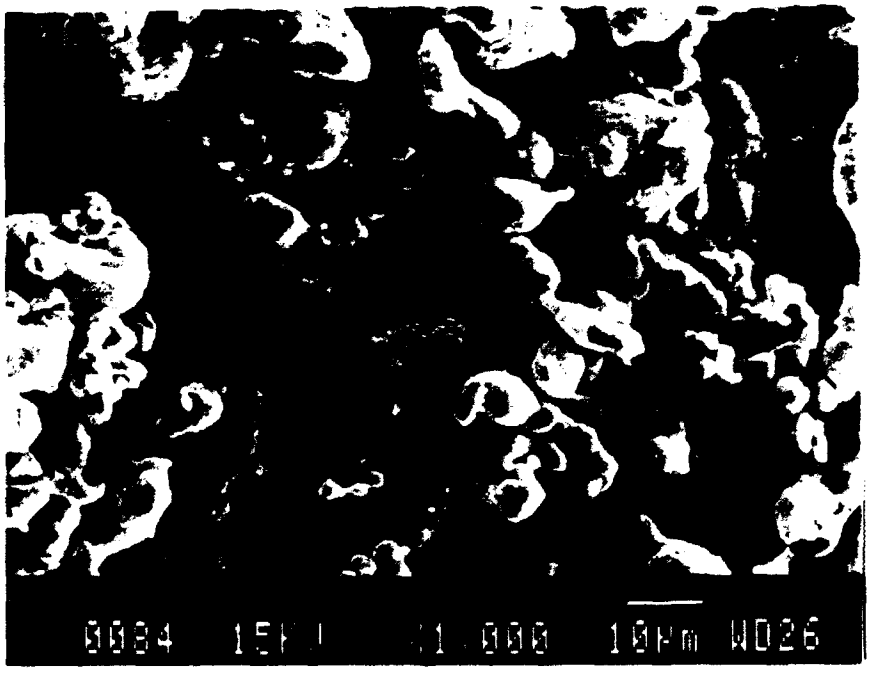

Figure D-2. Aluminum powder heterogeneous region at 1000X.

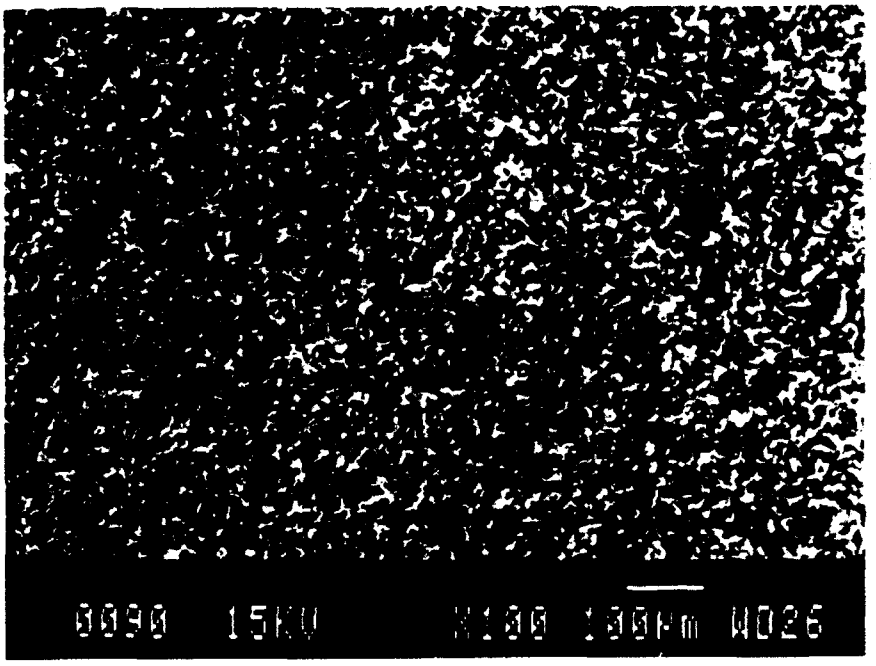

Figure D-3. Aluminum powder fine region at 100X.

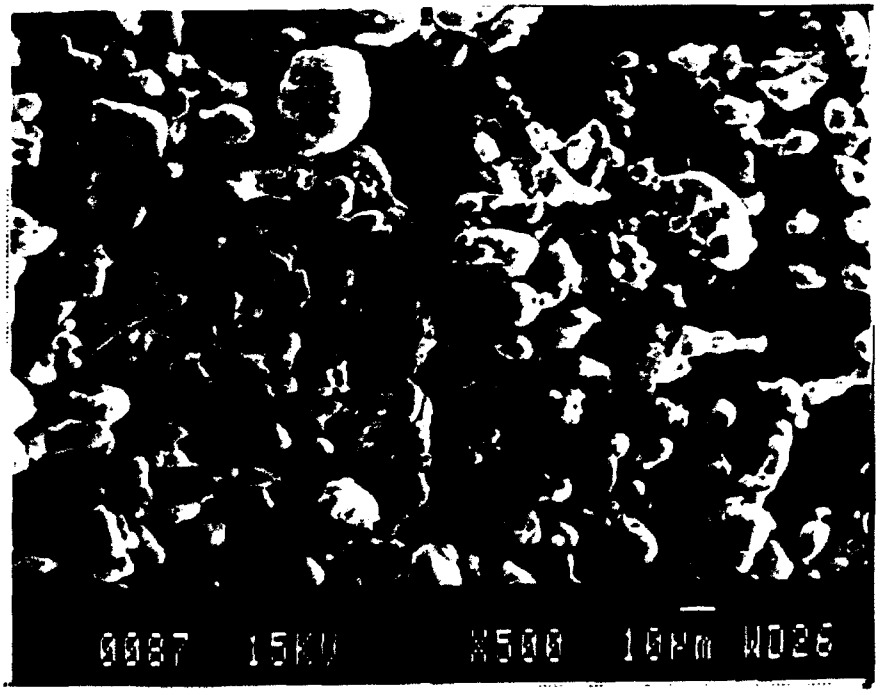

Figure D-4. Aluminum powder fine region at 500X.

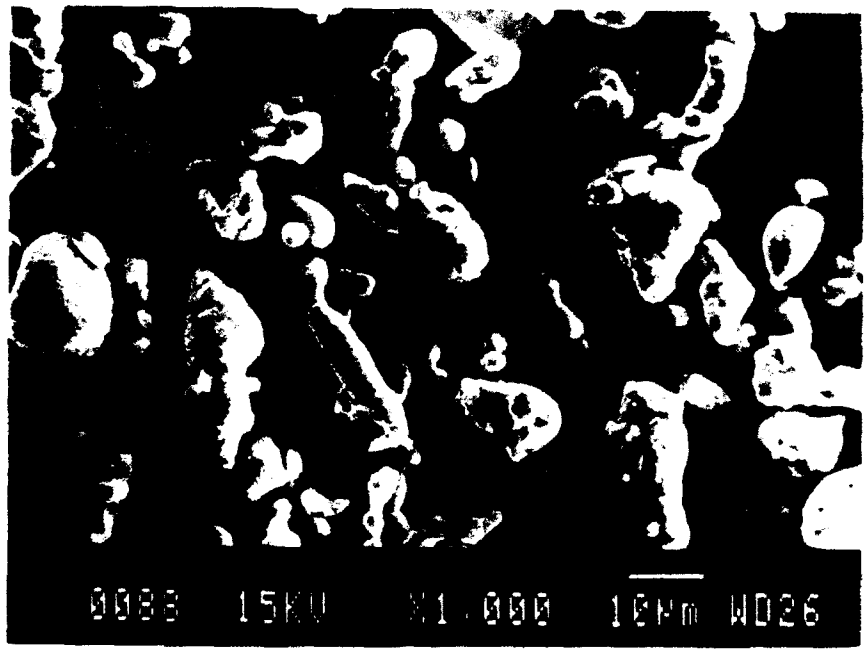

Figure D-5. Aluminum powder fine region at 1000X.

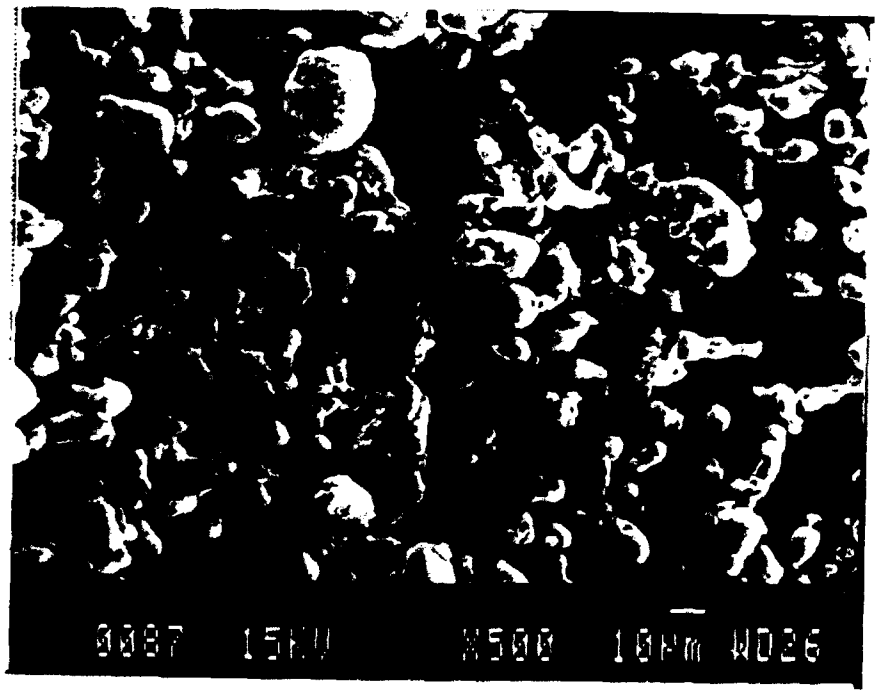

Figure D-6. Aluminum powder fine region at 1500X.

No. of Copies	Organization
2	Administrator Defense Technical Info Center ATTN: DTIC-DDA Cameron Station Alexandria, VA 22304-6145
1	Commander U.S. Army Materiel Command ATTN: AMCAM 5001 Eisenhower Ave. Alexandria, VA 22333-0001
1	Director U.S. Army Research Laboratory ATTN: AMSRL-OP-CI-AD, Tech Publishing 2800 Powder Mill Rd. Adelphi, MD 20783-1145
1	Director U.S. Army Research Laboratory ATTN: AMSRL-OP-CI-AD, Records Management 2800 Powder Mill Rd. Adelphi, MD 20783-1145
2	Commander U.S. Army Armament Research, Development, and Engineering Center ATTN: SMCAR-TDC Picatinny Arsenal, NJ 07806-5000
1	Director Benet Weapons Laboratory U.S. Army Armament Research, Development, and Engineering Center ATTN: SMCAR-CCB-TL Watervliet, NY 12189-4050
1	Director U.S. Army Advanced Systems Research and Analysis Office (ATCOM) ATTN: AMSAT-R-NR, M/S 219-1 Ames Research Center Moffett Field, CA 94035-1000
1 (Class. only)	Commander U.S. Army Missile Command ATTN: AMSMI-RD-CS-R (DOC) Redstone Arsenal, AL 35898-5010
1	Commander U.S. Army Tank-Automotive Command ATTN: AMSTA-JSK (Armor Eng. Br.) Warren, MI 48397-5000
1	Director U.S. Army TRADOC Analysis Command ATTN: ATRC-WSR White Sands Missile Range, NM 88002-5502
1 (Class. only)	Commandant U.S. Army Infantry School ATTN: ATSH-CD (Security Mgr.) Fort Benning, GA 31905-5660
1 (Unclass. only)	Commandant U.S. Army Infantry School ATTN: ATSH-WCB-O Fort Benning, GA 31905-5000
	Aberdeen Proving Ground
2	Dir, USAMSAA ATTN: AMXSY-D AMXSY-MP, H. Cohen
1	Cdr, USATECOM ATTN: AMSTE-TC
1	Dir, USAERDEC ATTN: SCBRD-RT
1	Cdr, USACBDCOM ATTN: AMSCB-CII
1	Dir, USARL ATTN: AMSRL-SL-I
5	Dir, USARL ATTN: AMSRL-OP-AP-L

2 Under Secretary of Defense for Research and Engineering
ATTN: TWP/OM
T. Hitchcock
Washington, DC 20301-3100

2 Director
Defense Advanced Research Projects Agency
ATTN: Technical Library
T. Hafner
3701 North Fairfax Drive
Arlington, VA 22203-1714

1 Director
Defense Intelligence Agency
ATTN: Technical Library
Washington, DC 20301

6 Commander
Defense Nuclear Agency
ATTN: T. Kennedy
C. McFarland
C. Gallaway
E. Patnaik
R. Rohr
G. Ullrich
M. Holm
Washington, DC 20305-1000

1 HQDA (DAEN-RDZ-A)
Washington, DC 20310-1000

1 HQDA (DAEN-RDM)
Washington, DC 20310-1000

1 HQDA (SARD-TR/Ms. K. Kimonos)
Washington, DC 20310-0103

1 HQDA (SARD-TR/Dr. R. Chait)
Washington, DC 20310-1030

1 HQDA (SARD-TT/Ms. C. Nash)
Washington, DC 20310-0103

1 HQDA (SARD-TT/Dr. F. Milton)
Washington, DC 20310-1030

1 Natick RD&E Center
ATTN: F. Bissett
PSD/SATD
STRNC-YS
Kansas Street
Natick, MA 01760-5020

2 Commander
U.S. Army Training & Doctrine Command
ATTN: Technical Library
ATCD-G, M. Pastel
Fort Monroe, VA 23651

3 Commander
U.S. Army Armament RD&E Center
ATTN: SMCAR-AEE-WW
Pai Lu
N. Slagg
J. Pearson
Picatinny Arsenal, NJ 07806-5000

10 Commander
U.S. Army Belvoir RD&E Center
ATTN: Technical Library
STRBE-N, Heberlein
STRBE-NA, Weaver
STRBE-BLORE
STRBE-CFLO
STRBE-NE (3 cys)
STRBE-ND, Spitzer
STRBE-NDM, Dillon
Fort Belvoir, VA 22060-5606

18 Director
U.S. Army Research Laboratory
ATTN: AMSRL-SS-FF,
J. Gerber
T. Pham
M. Fong
K. Tran
AMSRL-WT-N,
J. Gwaltney
J. Ingram
J. McGarrity
AMSRL-WT-NA, R. Kehs
AMSRL-WT-NB, M. Abe
AMSRL-WT-ND, J. Miletta
AMSRL-WT-NF, L. Jasper
AMSRL-WT-NG, T. Oldham
AMSRL-WT-NH, J. Corrigan
AMSRL-SL-C, J. Hughes
AMSRL-SL-CN,
S. Share
E. Fioravante
R. Lingebach
2800 Powder Mill Road
Adelphi, MD 20783-1145

3 Director
U.S. Army Research Laboratory
ATTN: Technical Library
AMSRL-MA-PA,
W. Haskell
E. Rigas
Watertown, MA 02172-0001

1 Commander
U.S. Army White Sands Missile Range
ATTN: STEW-NED, J. Meason
White Sands Missile Range, NM 88002

2 Commander
U.S. Army Tank Automotive Command
ATTN: Technical Library
AMFTA-RSA, T. Meitzler
Warren, MI 48397-5000

2 Commander
U.S. Army Nuclear and Chemical Agency
ATTN: Technical Library
G. Long
D. Bach
7150 Heller Loop, Suite 101
Springfield, VA 22150-3198

2 Commander
U.S. Army Concepts Analysis Agency
ATTN: Technical Library
M. Ogorzalek
8120 Woodmont Ave.
Bethesda, MD 20814

1 Commander
U.S. Army Research Office
ATTN: Technical Library
P.O. Box 12211
Research Triangle Park, NC 27709

3 Commander
U.S. Army Foreign Science and
Technology Center
ATTN: T. Reeder
G. Goodwin
Technical Library
220 7th St., NE
Charlottesville, VA 22901-5396

1 Commander
U.S. Army Dugway Proving Ground
ATTN: Technical Library
Dugway, UT 84022

2 U.S. Army Corps of Engineers
Construction Engineering Research
Laboratory
ATTN: Technical Library
C. Herring
P.O. Box 9005
Champaign, IL 61826-9005

11 U.S. Army Engineer Waterways
Experiment Station
ATTN: Technical Library
M. Ford
K. Davis
D. Rickman
J. Stout
J. Ingram
R. Dinan
G. McMahon
P. King
C. Joachim
B. Armstrong
P.O. Box 631
Vicksburg, MS 39180-0631

1 Commandant
U.S. Army Engineer School
ATTN: Technical Library
Fort Leonard Wood, MO 65473

1 Commander
U.S. Army Cold Regions R & E Lab
ATTN: Technical Library
P.O. Box 282
Hanover, NH 03755

1 U.S. Army Corps of Engineers
Omaha District
ATTN: D. Nebuda
Mail Code CEMRO-ED-SH
215 N. 17th Street
Omaha, NE 68102-4978

7 Officer In Charge
Dahlgren Division, Detachment White Oak
Naval Surface Warfare Center
ATTN: Technical Library
F. Warnock
R. Ferguson
K. Chien
J. Collins
R. Persh
M. Ruppalt
10901 New Hampshire Rd.
Silver Spring, MD 20903-5640

3 Commander
Dahlgren Division
Naval Surface Warfare Center
ATTN: Technical Library
L. Fontenot
J. Brown
17320 Dahlgren Road
Dahlgren, VA 22448-5000

2 Commander
Naval Surface Warfare Center
Carderock Division
ATTN: Technical Library
M. Orr
Code 1101
Philadelphia, PA 19112-5083

2 Commander
Naval Research Laboratory
ATTN: Technical Library
William A. Schmidt
Washington, DC 20375

1 Commander
Naval Surface Warfare Center
ATTN: Technical Library
Silver Spring, MD 20903-5000

1 Commander
Naval Weapons Center
ATTN: Technical Library
China Lake, CA 93555-6001

1 Officer-In-Charge
Naval EOD Facility
ATTN: Technical Library
Indian Head, MD 20640

4 Commander
Naval Coastal Systems Center
ATTN: R. Denton
C. Wicke
MAJ Cutchall
Technical Library
Panama City, FL 32407

2 Director
Nuclear Effects Directorate
ATTN: Technical Library
J. Briones
White Sands Missile Range, NM 88002

2 Commander
Marine Corps RD&E Command
ATTN: D. Vaughn
Technical Library
Quantico, VA 22134-5080

1 USAF Systems Command
ATTN: Technical Library
Andrews AFB, MD 20334

2 USIA,World Net
ATTN: Technical Library
J. Ryan
Rm. 2410 Patrick Henry Building
601 D St. NW
Washington, DC 20547

1 Phillips Laboratory
ATTN: Technical Library
Kirtland AFB, NM 87118-6008

4 Field Command, DNA
ATTN: LCDR Z. Myers
CPT M. Scott
J. Renick
E. Martinez (2 cys)
Kirtland AFB, NM 87115-5000

1 AFOSR
ATTN: Technical Library
Bolling AFB, DC 20332

3 WL/MNME
ATTN: G. Parsons
J. Foster
Technical Library
Eglin AFB, FL 32542-5000

1 Director
NASA-Science Technical International
Facility
P.O. Box 8754
BWI Airport, MD 21240

1 NOAA, Oceanic and Atmospheric Research
ATTN: CPT Smart
W. Callender
1335 East-West Hwy
SSMC3, Mailcode R/PDC
Silver Spring, MD 20910

1 OIR/CSD/CRB
ATTN: A. M. Jones
Rm 1413, OHB
Washington, DC 20505

1 Director
Idaho National Laboratory
ATTN: Technical Library
P.O. Box 1625
Idaho Falls, ID, 83415

1 Director
Los Alamos National Laboratory
ATTN: Technical Library
P.O. Box 1663
Los Alamos, NM 87545

4 Director
Sandia National Laboratories
ATTN: Technical Library
R. Ostensen
S. Snyder
M. Sagartz
P.O. Box 5800
Albuquerque, NM 87185

1 Director
Lawrence Livermore National Laboratory
ATTN: Technical Library
A. Kuhl
P.O. Box 808
Livermore, CA 94550

2 Aberdeen Research Center
ATTN: J. Keefer
N. Ethridge
P.O. Box 548
Aberdeen, MD 21001

2 Advanced Technology and Research Inc.
ATTN: Technical Library
J. Gott
14900 Swietzer Lane
Laurel, MD 20707

1 Aerospace Corporation
ATTN: Technical Library
P.O. Box 92957
Los Angeles, CA 90009

1 Alcan Powders and Chemicals
ATTN: Technical Library
P.O. Box 290
Elizabeth, NJ 07207

3 Allied Contracters, Inc.
ATTN: Technical Library
T. Crawford
A. Simpson
204 East Preston Street
Baltimore, MD 21202

1 The Aluminum Association, Inc.
ATTN: Technical Library
818 Connecticut Ave. N.W.
Washington, DC 20006

1 Aluminum Company of America
ATTN: Technical Library
1501 Alcoa Building
Pittsburg, PA 15219

1 AMPAL
ATTN: Technical Library
P.O. Box 31
Flemington, NJ 08822

2 Anser, Missile Division
ATTN: Technical Library
R. Leginus
Crystal Gateway 3
1215 Jefferson Davis Highway
Arlington, VA 22202

1 Applied Research Associates, Inc.
ATTN: R. Florey
2750 Eisenhower Ave., Suite 104
Alexandria, VA 22314

2 Applied Research Associates, Inc.
ATTN: R. Guice
R. Heyman
5941 S. Middlefield Road
Littleton, CO 80123

1 Applied Research Associates, Inc.
ATTN: J. Drake
3202 Wisconson Ave.
Vicksburg, MS 39180

1 Atlantic Research Corporation
ATTN: Technical Library
5390 Cherokee Ave.
Alexandria, VA 22314

1 Atomized Metal Powders Inc.
ATTN: Technical Library
25 East 39th Street
New York, NY 10016

1 Battelle
TWSTIAC
505 King Ave.
Columbus, OH 43202-2093

1 BDM Corporation
ATTN: Technical Library
7915 Jones Branch Drive
McLean, VA 22102

2 Boeing Helicopters
ATTN: Technical Library
J. Cosgrove
P.O. Box 16858, MS P30-07
Philadelphia, PA 19142-0858

2 Boeing Military Airplane Comany
ATTN: Technical Library
R. Lorenz
P.O. Box 7730
Wichita, KS 67277-7730

1 Booz-Allen & Hamilton Inc.
ATTN: Technical Library
Crystal Square 2, Suite 1100
1725 Jefferson Davis Hwy
Arlington, VA 22202-4158

2 Denver Research Institute
ATTN: Technical Library
L. Brown
P.O. Box 10127
Denver, CO 80210

2 Dynamic Science, Inc.
ATTN: S. Zardas
P. Neuman
P.O. Box N
Aberdeen, MD 21001

2 Electrospace Systems, Inc.
ATTN: Technical Library
S. Parekh
P.O. Box 831359
Richardson, TX 75083-1359

1 EMTEC Systems, Inc.
ATTN: J. Lattery
4500 Anaheim Ave, NE B-6
Albuquerque, NM 87113

1 Ethyl Corporation
ATTN: Technical Library
Houston Plant, Box 472
Pasadena, TX 77501

1 FMC Corporation
ATTN: Technical Library
1105 Coleman Ave.
San Jose, CA 95108

1 Franklin Research Center
ATTN: Technical Library
Benjamin Franklin Parkway
Philadelphia, PA 19103

2 General Sciences, Inc.
ATTN: Technical Library
M. Riley
655 S. Gravers Road
Plymouth Meeting, PA 19462

3 IRT Corporation
ATTN: Technical Library
V. DePenger
C. Schuck
101 S. Kreamer Blvd.
Suite 132
Placentia, CA 92670

1 ITT Research Institute
ATTN: Technical Library
10 West 35th Street
Chicago, IL 60616

2 ITT Aerospace/Optical Division
ATTN: Technical Library
K. Ruster
3700 East Pontiac Street
P.O. Box 3700
Fort Wayne, IN 46803

3 The Johns Hopkins University
Applied Physics Laboratory
ATTN: Technical Library
T. Coughlin
J. Kouroupis
Johns Hopkins Road
Laurel, MD 20707

1 Kaman Sciences Corporation
ATTN: F. McMullan
6400 Uptown Blvd, Suite 300E
Albuquerque, NM 87110

1 The Kaempfer Company
ATTN: W. Herman
1150 18th Street, N.W.
Suite 1000
Washington, D.C. 20036

2 Martin Marietta Aerospace
ATTN: Technical Library
M. Bauer
P.O. Box 179
Denver, CO 80201

2 McDonnell Douglas Corp.
ATTN: Technical Library
C. Corey
Ballistic Missile Defense
5301 Bolsa Avenue
Hunington Beach, CA 92647

1 Medtherm Corporation
ATTN: Larry Jones
P.O. Box 412
Huntsville, AL 35804

2 New Mexico Engineering Research Institute
ATTN: Technical Library
R. Robey
University of New Mexico
Albuquerque, NM 87131-1376

2 Olin Ordnance
ATTN: Technical Library
J. Kibiger
Product/Material Control
10101-9th Street North
St. Petersburg, FL 33716

1 PCI
ATTN: V. Schmidt
900 19th St. NW
Suite 600
Washington D.C. 20006

2 Reynolds Metals Company
ATTN: Technical Library
N. Koopman
Plant #3, 4101 Camp Ground Rd.
Louisville, KY 40211

3 S-CUBED, Maxwell Laboratories
ATTN: Technical Library
C. Needham
K. Schnieder
Albuquerque, NM 87131

1 SI/Division of Spectrum 39
ATTN: W. Schuman
8831 Satyr Hill Rd, Suite 312
Baltimore, MD 21234

2 Science Applications International Corp.
ATTN: Technical Library
J. Bryars
11526 Sorrento Valley Road
Suite A
San Diego, CA 92121

4 Science Applications International Corp.
ATTN: J. Simmons
J. Guest
J. Dishon
P. Versteegan
P.O. Box 1303
1710 Goodrich Dr.
McLean, VA 22102

1 Science Applications International Corp.
ATTN: S. Doerr
2109 Air Park Rd., SE
Albuquerque, NM 87106

1 Silberline Manufacturing Company, Inc.
ATTN: Technical Library
P.O. Box A
Lansford, PA 18232

2 Simula Government Products Inc.
ATTN: Technical Library
W. Perciballi
10016 S. 51 st Street
Phoenix, AZ 85044-5299

1 Southwest Research Institute
ATTN: Technical Library
P.O. Drawer 28510
San Antonio, TX 78284

1 SRI International
ATTN: Technical Library
333 Ravenswood Ave.
Menlo Park, CA 94025

2 Tech Reps., Inc.
ATTN: F. McMullen
B. Collins
5000 Marble, N.E., Suite 222
Albuquerque, NM 87110

1 Teledyne McCormick Selph
ATTN: C. Garrison
P.O. Box 6
Hollister, CA 95023-0006

1 TERA
New Mexico Institute of Technology
ATTN: Technical Library
Socorro, NM 87801

1 Thermogage, Inc
ATTN: Charles Brookly
330 Alleghany St.
Frostburg, MD 21532

1 Transmet Corporation
ATTN: Technical Library
4290 Perimeter Dr.
Columbus, OH 43228

1 U.S. Bronz Powders. Inc.
ATTN: Technical Library
P.O. Box 31
Route 202
Flemington, NJ 008822

2 University of Maryland at College Park
Department of Mechanical Engineering
ATTN: ENME,
J. Duncan
J. Wallace
Rm. 2168
Engineering Classroom Building
College Park, MD 20742-5121

1 Valimet, Inc.
ATTN: Technical Library
431 East Sperry Road
Stockton, CA 95206

4 Walcoff and Associates, Inc.
ATTN: T. Toya
C. Paquette
C. Walcoff
R. Walden
635 Slaters Lane
Alexandria, VA 22314

Aberdeen Proving Ground

1 Cmd, AMCCOM
ATTN: SMCAR-ACW
Weapons Systems Concept Team
Bldg. E3516

9 Dir, USAMSAA
ATTN: AMSXB-GB, Abel
AMXSY-S, Carroll
AMXSY-GC,
B. Bramwell
C. Eissner
L. Meredith
W. Wiederman
A. Wong
LTC Hassell
JTCG-ME, LaGrange

2 Cmd, USACSTA
ATTN: STECS-AE-TL, Bindel
STECS-AE-TH, Wiley

7 Dir, ERDEC
ATTN: SCDRB-RTT,
L. Bickford
K. Fritz
S. Funk
G. Goldsmith
R. Milecki
I. Swann
A. Turetsky

1 Cmdr, USAOC&S
ATTN: Technical Library

6 Cmdr, USATECOM
ATTN: AMSTE-SI-F
AMSTE-CL
AMSTE-EV-O
AMSTE-TA-F
AMSTE-ML
AMSTE-TE-V

73 Dir, U.S. Army Research Laboratory
ATTN: AMSRL-CI-S, A. Mark
AMSRL-CP-TI, J. Polk
AMSRL-WT-TD, P. Kingman
AMSRL-WT-NC,
R. Lottero
R. Loucks (40 cys)
P. Muller (10 cys)
R. Thane (10 cys)
J. Sullivan
R. Raley
W. Wright
G. Fergeson
S. Schramel
K. Opalka
C. Mermagen
AMSRL-WT-WG, L. Puckett

2 Bundesamt für Wehrtechnik and Beschaffung
ATTN: K. Köhler
Technical Library
Postfach 7360
5400 Kolenz, Germany

2 Defense Research Establishment Suffield
ATTN: D. Ritzel
Technical Library
P.O. Box 4000
Medicine Hat
Alberta, T1A 8K6 Canada

4 DSTO, Materials Research Laboratory
ATTN: N. Burman
D. Saunders
M. Buckland
Technical Library
P.O. Box 50
Ascot Vale
Victoria, Australia 3032

2 Fraunhofer-Institut für Kurzzeitdynamik
Ernst Mach Institut
ATTN: H. Amann
Technical Library
7800 Freiburg, Germany

2 Industrieanlagen-Betriebsgesellschaft mbH
ATTN Technical Library
H. Diekhoff
Abteilung Finite Berechnungsverfahren
Einsteinstraße 20, D-8012 Ottobrunn

7 Ministry of Defense
Atomic Weapons Establishment
ATTN: M. German
J. Threadgold
W. Babbage
B. Bogartz
I. Smith
J. Tate
M. King
Technical Library
Foulness, Essex, SS3 9XE, UK

4 Ministre de la Defense
Centre d'Etude de Gramat
ATTN: S. Gratias
E. Canton
D. Mergnat
Technical Library
46500 Gramat, France

2 Ministere de l'Equipment
Laboratoire d'Essais d'Equipements d'Abris
ATTN: Technical Library
D. Fau
Base de Viroulou - Alvignac
46500 Gramet, France

2 National Defense Research Institute
Weapons Technology Department
ATTN: H. Axelsson
Technical Library
P.O. Box 98
S-147 00 TUMBA, Sweden

3 Norwegian Defense Construction Service
Test and Development Section
ATTN: Technical Library
A. Jenssen
Oslo mil/Akershus
Oslo, Norway

1 Stores and Clothing Research and Development Establishment
ATTN: S. Elton
S. Cross
Technical Library
Flagstaff Rd.
Essex, C02 7SS, UK

2 Wehrwissenschaftliche Dienstselle für Sprengmittel und Sondertechnik
ATTN: M. Klaus
L. Klubert
Technical Library
Oberjettenberg
8230 Schneizlreuth, Germany

2 Wehrwissenschaftliche Dienstselle der Bundeswehr für ABC-Schutz
ATTN: W. Rehmann
Technical Library
Humboltstraße/Postfach 1142
3042 Münster, Germany

1 Dewey McMillan & Associates, Ltd.
ATTN: J. Dewey
1741 Feltham Road
Victoria, BC V8N 2A4, Canada

INTENTIONALLY LEFT BLANK.

USER EVALUATION SHEET/CHANGE OF ADDRESS

This Laboratory undertakes a continuing effort to improve the quality of the reports it publishes. Your comments/answers to the items/questions below will aid us in our efforts.

1. ARL Report Number ARL-TR-501 Date of Report August 1994

2. Date Report Received _____

3. Does this report satisfy a need? (Comment on purpose, related project, or other area of interest for which the report will be used.) _____

4. Specifically, how is the report being used? (Information source, design data, procedure, source of ideas, etc.) _____

5. Has the information in this report led to any quantitative savings as far as man-hours or dollars saved, operating costs avoided, or efficiencies achieved, etc? If so, please elaborate. _____

6. General Comments. What do you think should be changed to improve future reports? (Indicate changes to organization, technical content, format, etc.) _____

CURRENT ADDRESS

_____
Organization

_____
Name

_____
Street or P.O. Box No.

_____
City, State, Zip Code

7. If indicating a Change of Address or Address Correction, please provide the Current or Correct address above and the Old or Incorrect address below.

OLD ADDRESS

_____
Organization

_____
Name

_____
Street or P.O. Box No.

_____
City, State, Zip Code

(Remove this sheet, fold as indicated, tape closed, and mail.)
(DO NOT STAPLE)

DEPARTMENT OF THE ARMY

OFFICIAL BUSINESS

NO POSTAGE
NECESSARY
IF MAILED
IN THE
UNITED STATES

BUSINESS REPLY MAIL
FIRST CLASS PERMIT NO 0001, APG, MD

Postage will be paid by addressee

Director
U.S. Army Research Laboratory
ATTN: AMSRL-OP-AP-L
Aberdeen Proving Ground, MD 21005-5066